INFORMATION TO USERS

This manuscript has been reproduced from the microfilm master. UMI films the text directly from the original or copy submitted. Thus, some thesis and dissertation copies are in typewriter face, while others may be from any type of computer printer.

The quality of this reproduction is dependent upon the quality of the copy submitted. Broken or indistinct print, colored or poor quality illustrations and photographs, print bleedthrough, substandard margins, and improper alignment can adversely affect reproduction.

In the unlikely event that the author did not send UMI a complete manuscript and there are missing pages, these will be noted. Also, if unauthorized copyright material had to be removed, a note will indicate the deletion.

Oversize materials (e.g., maps, drawings, charts) are reproduced by sectioning the original, beginning at the upper left-hand corner and continuing from left to right in equal sections with small overlaps. Each original is also photographed in one exposure and is included in reduced form at the back of the book.

Photographs included in the original manuscript have been reproduced xerographically in this copy. Higher quality 6" x 9" black and white photographic prints are available for any photographs or illustrations appearing in this copy for an additional charge. Contact UMI directly to order.

UMI

A Bell & Howell Information Company
300 North Zeeb Road, Ann Arbor MI 48106-1346 USA
313/761-4700 800/521-0600

Université d'Ottawa · University of Ottawa

Free Vibration Analysis of Rectangular Mindlin Plates Resting on Uniform Elastic Edge Supports by the Superposition Method

Thesis Submitted to the School of Graduate Studies as Partial Fulfilment of the Requirements for the Degree of Master of Applied Science

By

Hai Qi

Department of Mechanical Engineering
Ottawa-Carleton Institute for Mechanical and Aerospace Engineering
University of Ottawa
Ottawa, Ontario, Canada
K1N 6N5

March, 1997

Abstract

In the present study, it is demonstrated that the traditional superposition method lends itself successfully to obtaining of eigenvalues and mode shapes for rectangular shear deformable plates resting on uniform elastic edge supports. The effect of transverse shear deformation is taken into account by means of the first order shear deformation relationship developed by Mindlin. Uniform elastic rotational and translational supports of any stiffness magnitudes are considered to act simultaneously along the four edges. The effects of twisting edge restraint are investigated for the first time. The governing differential equations are satisfied exactly throughout the plate domain. Eigenvalues are tabulated for the first six vibration modes of square plates with identical stiffnesses along all edges. It is shown that all the three classical boundary conditions, namely, free, simply supported, and clamped, are approached when the stiffness coefficients are allowed to take on appropriate limits. These appear to be the first analytical solutions to these important elastically supported plate vibration problems obtained by the superposition method.

Acknowledgments

The author would like to express his deep appreciation for the guidance and assistance that he has received from his supervisor Dr. D. J. Gorman. Without his years of experience in the field of plate vibration and his countless thoughtful suggestions and ideas, this work would not have been possible.

Special thanks also go to members of the Department of Mechanical Engineering, University of Ottawa, for their support and cooperation.

Finally, the author wishes to thank his wife, Jiangfeng Wu, for her love, patience, understanding and encouragement while this work was being completed.

Contents

Nomenclature

a, b	plate dimensions in x and y directions, respectively
D	flexural rigidity, $D = Eh^3/12(1 - \nu^2)$
E	Young's modulus
G	shear modulus
h	plate thickness
K	actual number of terms used in series of Levy type solutions
L	elastic translational stiffness along plate edge
R	elastic bending stiffness along plate edge
T	elastic twisting stiffness along plate edge
K_L	dimensionless translational stiffness along plate edge, $K_L = L/\kappa^2 G\phi_h$
K_R	dimensionless bending stiffness coefficient along plate edge, $K_R = R\phi a/D$ when $\eta = 0, 1$, $K_R = Ra/D$ when $\xi = 0, 1$
K_T	dimensionless twisting stiffness along plate edge, $K_T = 2aT/D(1 - \nu)$
M_x, M_y, M_{xy}	bending and twisting moments
M_ξ, M_η, $M_{\xi\eta}$	dimensionless bending and twisting moments
Q_x, Q_y	shear forces on planes x = const. And y = const., respectively
Q_ξ, Q_η	dimensionless shear forces
u, v, w	displacements in x, y, and z directions, respectively
W	lateral displacements divided by side length a
x, y, z	Cartesian coordinates
ξ	dimensionless in-plane coordinate, $\xi = x / a$
η	dimensionless in-plane coordinate, $\eta = y / a$
ϕ	plate aspect ratio, $\phi = b / a$
ϕ_h	plate thickness-to-length ratio, $\phi_h = h / a$
ρ	plate density per unit area

ψ_x, ψ_y	rotations with respect to x and y, respectively
ψ_ξ, ψ_η	rotations with respect to ξ and η , respectively
ε_x, ε_y, γ_{xy}	
γ_{yz}, γ_{zx}	plate strain components
σ_x, σ_y, τ_{xy}	
τ_{yz}, τ_{zx}	plate stress components
ν	Poisson ratio
κ^2	shear correction factor
ω	circular frequency of plate free vibration
λ^2	eigenvalue of plate free vibration, $\lambda^2 = \omega a^2\sqrt{\rho/D}$

List of Figures

Figure B.7. Sixth vibration mode shape of a thicker square plate ($\phi_h = 0.1$, $K_T = 0$, $K_R = K_L = 10$, $\lambda^2 = 86.82$).

List of Tables

Chapter 1

Introduction

1.1 Literature Review

In recent years, numerous advances have been made in connection with free vibration of thick plates, and a wide variety of plate theories as well as analytical techniques have been developed. Many numerical methods, such as the finite element method and the boundary element method, have also been used successfully in this area. A review of existing literature on the vibration analysis of thick plates can be found in [1]. In this thesis, reference will only be made to those publications which are considered to have direct relevance to problems under discussion and their solutions.

It is well known that results obtained by means of classical plate theory based on the Kirchhoff hypothesis are not truly applicable to plate vibration problems when the plate length-to-thickness ratio falls below certain levels. The Kirchhoff hypothesis assumes that straight lines originally normal to the plate median surface remain straight and normal during the deformation process. This simplifies the problem considerably but produces errors since the effects of transverse shear deformation are neglected. The classical plate theory overestimates the vibration frequencies of thick plates since the plate flexibility is underestimated. This phenomenon was well recognized by many researchers, like Reissner [2] and Mindlin [3]. Based on discarding the Kirchhoff hypothesis and incorporating transverse shear deformation effects, many refined plate theories, ranging from the first order Mindlin plate theory, the modified Mindlin theories to various higher order plate theories, were subsequently developed. It was Mindlin who first developed a mathematical free vibration formulation of the thick plate problem which not only incorporated the effects of deformation associated with transverse shear but also considered the effects of rotary inertia of the plate elements.

In the vibration analysis of isotropic moderately thick plates, the first order Mindlin theory will usually suffice. A comparison prepared by Yu and Cleghorn [4] indicates that there is excellent agreement between the results obtained by using the Mindlin plate theory and those by the higher order plate theories. Therefore, the Mindlin plate theory is adopted in this study.

In the Mindlin plate theory, any straight line originally normal to the plate median surface will, during deformation, remain straight but not generally normal to the plate median surface. In the true situation such a line is generally curved but the assumed straight non-normal line can well approximate this curved line in an average sense at all points. One can think of the work of Mindlin as an extension of the Timoshenko thick beam theory to the two dimensional rectangular plate problem. Although in the theory, a constant shear stress distribution through the thickness is assumed, it can give reasonably accurate solutions when used in conjunction with a shear correction factor k on the shear modulus.

The superposition method for free vibration analysis has been used with considerable success to obtain accurate solutions to numerous thin plate free vibration problems. These solutions have been widely reported in the literature with the principal reference being the work of Gorman [5]. More recently, the superposition method has been employed to analyze completely free Mindlin plates by Gorman and Ding [6] [7] and Mindlin plates with combinations of clamped and simply supported edge conditions by Yu and Cleghorn [4] [8] [9].

An attractive feature of the superposition method centers around the fact that, unlike the Rayleigh-Ritz method which is often employed by many researchers in their papers, no shape functions need to be selected to represent the deformed plate. Exact Levy type solutions are obtained for rectangular plate forced vibration problems(building blocks). Each building block is driven by a harmonic moment or force distributed along one edge. After superimposing these solutions, Fourier coefficients appearing therein are adjusted in order to satisfy the various boundary conditions. All solutions obtained by the superposition method satisfy the governing differential equations exactly throughout the domain of the plate. The boundary conditions are satisfied to any desired degree of accuracy.

1.2 Motivation and Objectives

It is generally accepted that edge support provided along the boundaries of rectangular plates is always elastic in nature. One may, for convenience, choose to idealize such support as being of the classical clamped or simple support type, but it is recognized that such idealized conditions are never fully achieved in reality. The achieving of such conditions would imply infinite stiffness in the support structure. Research studies for non-classical boundaries therefore need to be emphasized.

Reviewing the literature, it is noticed that very little has been done regarding free vibration of thick rectangular plates resting on uniform elastic edge supports since Mindlin established the improved plate theory. Only two works are found in this area, one is due to Chung, Chung and Kim [10] who have considered orthotropic Mindlin plates with edges elastically restrained against bending rotation using Rayleigh-Ritz method, another is done by Saha, Kar and Datta [11] who have used a variational method to analyze rectangular Mindlin plates with elastic translational and rotational (bending) restraints uniformly distributed along the edges.

Activated by the work of Gorman [12] regarding the free vibration of rectangular thin plates with uniform elastic edge supports, in this thesis, the superposition method is further exploited to obtain solutions for the natural frequencies and mode shapes of rectangular Mindlin plates resting on uniform elastic edge supports. All the three types of elastic supports, rotational (bending and twisting) and translational, are considered. To the author's knowledge, those solutions represent the first analytical solutions to be achieved for these challenging problems by the superposition method.

Chapter 2

The Underlying Theory

In this chapter, the dimensionless governing differential equations for free vibration analysis of thick isotropic plates, based on Mindlin plate theory, are developed for the sake of completeness. Also, the associated various boundary conditions will be presented.

2.1 Governing Differential Equations

The rectangular plate is referred to an x, y, z system of rectangular coordinates shown in Figure A.1. The faces of the plate are the planes $z = \pm h / 2$. The notation for plane stress and strain components as well as materials properties are defined in customary manner [3].

Considering the general Hooke's law for isotropic materials in three-dimensional elasticity theory with the expressions for the six components of strain in term of six components of stress. Of the six equations, the one containing unit elongation, ε_z, normal to the faces of the plate is dropped, and σ_z is also neglected. The remaining five equations are then solved for stress components σ_x, σ_y, τ_{xy}, τ_{zx}, τ_{yz} in terms of strain components ε_x , ε_y, γ_{xy}, γ_{zx}, γ_{yz}. We obtain the following plate stress-strain relationship

$$\sigma_x = \frac{E}{1 - \nu^2} (\varepsilon_x + \nu \varepsilon_y),$$

$$\sigma_y = \frac{E}{1 - \nu^2} (\varepsilon_y + \nu \varepsilon_x),$$

$$\tau_{xy} = G\gamma_{xy}, \tag{2.1}$$

$$\tau_{zx} = G\gamma_{zx},$$

$$\tau_{yz} = G\gamma_{yz}.$$

From the three-dimensional elasticity theory, we also have the following plate strain-displacement relationships by ignoring the equation containing strain ε_z

$$\varepsilon_x = \frac{\partial u}{\partial x},$$

$$\varepsilon_y = \frac{\partial v}{\partial y},$$

$$\gamma_{xy} = \frac{\partial u}{\partial y} + \frac{\partial v}{\partial x}, \tag{2.2}$$

$$\gamma_{zx} = \frac{\partial u}{\partial z} + \frac{\partial w}{\partial x},$$

$$\gamma_{yz} = \frac{\partial w}{\partial y} + \frac{\partial v}{\partial z},$$

where u, v, w are plate displacements in x, y, z directions, respectively.

The plate bending and twisting moments and transverse shear forces, all per unit of length, are now defined as follows

$$M_x = \int_{-h/2}^{+h/2} \sigma_x z dz,$$

$$M_y = \int_{-h/2}^{+h/2} \sigma_y z dz,$$

$$M_{xy} = \int_{-h/2}^{+h/2} \tau_{xy} z dz, \tag{2.3}$$

$$Q_x = \int_{-h/2}^{+h/2} \tau_{zx} dz,$$

$$Q_y = \int_{-h/2}^{+h/2} \tau_{yz} dz.$$

It is assumed in the Mindlin plate theory that u and v are proportional to z and w is independent of z ,

$$u = z\psi_x(x,y,t),$$

$$v = z\psi_y(x,y,t), \tag{2.4}$$

$$w = w(x,y,t),$$

where ψ_x and ψ_y are the local rotations (change of slope) in the x and y directions, respectively, of lines originally normal to the plate before deformation.

Substituting equations (2.4) into strain-displacement equations (2.2), then into stress-strain equations (2.1), we obtain

$$\sigma_x = \frac{Ez}{1-\nu^2}\left(\frac{\partial \psi_x}{\partial x} + \nu\frac{\partial \psi_y}{\partial y}\right),$$

$$\sigma_y = \frac{Ez}{1-\nu^2}\left(\frac{\partial \psi_y}{\partial y} + \nu\frac{\partial \psi_x}{\partial x}\right),$$

$$\tau_{xy} = \frac{Ez}{2(1+\nu)}\left(\frac{\partial \psi_x}{\partial y} + \frac{\partial \psi_y}{\partial x}\right), \tag{2.5}$$

$$\tau_{zx} = G\,(\psi_x + \frac{\partial w}{\partial x}),$$

$$\tau_{yz} = G\,(\psi_y + \frac{\partial w}{\partial y}).$$

The first three of equations (2.5) are multiplied by z and integrated over the plate thickness, the last two are integrated over plate thickness directly. We finally achieve, after incorporating equations (2.3), the expressions for bending and twisting moments and shear forces in terms of plate displacements

$$M_x = D\,(\frac{\partial \psi_x}{\partial x} + \nu\frac{\partial \psi_y}{\partial y}),$$

$$M_y = D\,(\frac{\partial \psi_y}{\partial y} + \nu\frac{\partial \psi_x}{\partial x}),$$

$$M_{xy} = \frac{1-\nu}{2} D\,(\frac{\partial \psi_x}{\partial y} + \frac{\partial \psi_y}{\partial x}), \qquad (2.6)$$

$$Q_x = \kappa^2 Gh\,(\psi_x + \frac{\partial w}{\partial x}),$$

$$Q_y = \kappa^2 Gh\,(\psi_y + \frac{\partial w}{\partial y}),$$

where D is the plate modulus

$$D = \frac{Eh^3}{12(1-\nu^2)}, \qquad (2.7)$$

and κ^2 is the constant, introduced here as transverse shear correction coefficient.

Now, consider the well-known stress equation of motion of three-dimensional elasticity theory

$$\frac{\partial \sigma_x}{\partial x} + \frac{\partial \tau_{xy}}{\partial y} + \frac{\partial \tau_{zx}}{\partial z} = \frac{\rho}{h}\frac{\partial^2 u}{\partial t^2},$$

$$\frac{\partial \tau_{xy}}{\partial x} + \frac{\partial \sigma_y}{\partial y} + \frac{\partial \tau_{yz}}{\partial z} = \frac{\rho}{h}\frac{\partial^2 v}{\partial t^2},$$
$$\frac{\partial \tau_{xz}}{\partial x} + \frac{\partial \tau_{yz}}{\partial y} + \frac{\partial \sigma_z}{\partial z} = \frac{\rho}{h}\frac{\partial^2 w}{\partial t^2}, \tag{2.8}$$

where ρ is the mass per unit area.

The first two of equations (2.8) are multiplied by z and integrated over the plate thickness, and the third one is integrated over the plate thickness directly. After making use of equations (2.3), (2.4) and the condition that the plate is free of in plane forces, transverse external loading or body forces, and neglecting the stress σ_z, equations (2.8) become

$$\frac{\partial M_x}{\partial x} + \frac{\partial M_{xy}}{\partial y} - Q_x = \frac{\rho h^2}{12}\frac{\partial^2 \psi_x}{\partial t^2},$$
$$\frac{\partial M_{xy}}{\partial x} + \frac{\partial M_y}{\partial y} - Q_y = \frac{\rho h^2}{12}\frac{\partial^2 \psi_y}{\partial t^2}, \tag{2.9}$$
$$\frac{\partial Q_x}{\partial x} + \frac{\partial Q_y}{\partial y} = \rho\frac{\partial^2 w}{\partial t^2}.$$

Substituting equations (2.6) into equations (2.9), we finally get the governing differential equations for Mindlin plates

$$\kappa^2 Gh\left(\frac{\partial^2 w}{\partial x^2} + \frac{\partial^2 w}{\partial y^2} + \frac{\partial \psi_x}{\partial x} + \frac{\partial \psi_y}{\partial y}\right) = \rho\frac{\partial^2 w}{\partial t^2}, \tag{2.10}$$
$$\frac{D}{2}\left[2\frac{\partial^2 \psi_x}{\partial x^2} + (1-\nu)\frac{\partial^2 \psi_x}{\partial y^2} + (1+\nu)\frac{\partial^2 \psi_y}{\partial x \partial y}\right] - \kappa^2 Gh\left(\psi_x + \frac{\partial w}{\partial x}\right) = \frac{\rho h^2}{12}\frac{\partial^2 \psi_x}{\partial t^2},$$
$$\frac{D}{2}\left[2\frac{\partial^2 \psi_y}{\partial y^2} + (1-\nu)\frac{\partial^2 \psi_y}{\partial x^2} + (1+\nu)\frac{\partial^2 \psi_x}{\partial x \partial y}\right] - \kappa^2 Gh\left(\psi_y + \frac{\partial w}{\partial y}\right) = \frac{\rho h^2}{12}\frac{\partial^2 \psi_y}{\partial t^2}.$$

It is possible to express the displacement $w(x,y,t)$, edge rotations $\psi_x(x,y,t)$ and $\psi_y(x,y,t)$ as a product of two functions, respectively, one involving only the space coordinates x and y and another involving the time variable,

$$w(x,y,t) = w(x,y)T(t),$$

$$\psi_x(x,y,t) = \psi_x(x,y)T(t), \tag{2.11}$$

$$\psi_y(x,y,t) = \psi_y(x,y)T(t).$$

Substituting equations (2.11) into equations (2.10) and separating the variables, it can be shown that

$$T(t) = A\sin(\omega t + \alpha), \tag{2.12}$$

where ω is known as circular frequency, A and α represent the amplitude and the phase angle, respectively. For the sake of brevity, w, ψ_x and ψ_y will be used hereafter to represent the space functions, $w(x,y)$, $\psi_x(x,y)$ and $\psi_y(x,y)$. The equations (2.10) then become

$$\kappa^2 Gh\left(\frac{\partial^2 w}{\partial x^2} + \frac{\partial^2 w}{\partial y^2} + \frac{\partial \psi_x}{\partial x} + \frac{\partial \psi_y}{\partial y}\right) + \rho\omega^2 w = 0, \tag{2.13}$$

$$\frac{D}{2}\left[2\frac{\partial^2 \psi_x}{\partial x^2} + (1-\nu)\frac{\partial^2 \psi_x}{\partial y^2} + (1+\nu)\frac{\partial^2 \psi_y}{\partial x \partial y}\right] - \kappa^2 Gh\left(\psi_x + \frac{\partial w}{\partial x}\right) + \frac{\rho\omega^2 h^2}{12}\psi_x = 0,$$

$$\frac{D}{2}\left[2\frac{\partial^2 \psi_y}{\partial y^2} + (1-\nu)\frac{\partial^2 \psi_y}{\partial x^2} + (1+\nu)\frac{\partial^2 \psi_x}{\partial x \partial y}\right] - \kappa^2 Gh\left(\psi_y + \frac{\partial w}{\partial y}\right) + \frac{\rho\omega^2 h^2}{12}\psi_y = 0.$$

Experience has shown that it is always advantageous to use the non-dimensional governing differential equations. After introducing the following transformations [4]

$$\xi = \frac{x}{a},$$

$$\eta = \frac{y}{b},$$

$$W(\xi,\eta) = \frac{w(x,y)}{a},$$

$$\psi_\xi = \psi_x,$$

$$\psi_\eta = \psi_y, \tag{2.14}$$

$$M_\xi = \frac{M_x a}{D},$$

$$M_\eta = \frac{M_y b}{D},$$

$$M_{\xi\eta} = \frac{2M_{xy} a}{D(1 - \nu)},$$

$$Q_\xi = \frac{Q_x}{k^2 Gh},$$

$$Q_\eta = \frac{Q_y}{k^2 Gh}.$$

The non-dimensional governing differential equations for Mindlin plates may be written as

$$\begin{aligned}
&\frac{\partial^2 W}{\partial \xi^2} + \frac{1}{\phi^2}\frac{\partial^2 W}{\partial \eta^2} + \frac{\partial \psi_\xi}{\partial \xi} + \frac{1}{\phi}\frac{\partial \psi_\eta}{\partial \eta} + \frac{\lambda^4 \phi_h^{\,2}}{\nu_3} W = 0,\\
&\frac{\partial^2 \psi_\xi}{\partial \xi^2} + \frac{\nu_1}{\phi^2}\frac{\partial^2 \psi_\xi}{\partial \eta^2} + \frac{\nu_2}{\phi \nu_1}\frac{\partial^2 \psi_\eta}{\partial \xi \partial \eta} - \frac{\nu_3}{\phi_h^{\,2}}\left(\psi_\xi + \frac{\partial W}{\partial \xi}\right) + \frac{\lambda^4 \phi_h^{\,2}}{12}\psi_\xi = 0,\\
&\frac{\partial^2 \psi_\eta}{\partial \xi^2} + \frac{1}{\phi^2 \nu_1}\frac{\partial^2 \psi_\eta}{\partial \eta^2} + \frac{\nu_2}{\phi \nu_1}\frac{\partial^2 \psi_\xi}{\partial \xi \partial \eta} - \frac{\nu_3}{\phi_h^{\,2} \nu_1}\left(\psi_\eta + \frac{1}{\phi}\frac{\partial W}{\partial \eta}\right) + \frac{\lambda^4 \phi_h^{\,2}}{12\nu_1}\psi_\eta = 0,
\end{aligned} \tag{2.15}$$

where

$$\phi_h = \frac{h}{a},$$

$$\nu_1 = \frac{(1 - \nu)}{2},$$

$$\nu_2 = \frac{(1 + \nu)}{2}, \tag{2.16}$$

$$\nu_3 = 6\kappa^2(1 + \nu),$$

$$\lambda^2 = \omega a^2\sqrt{\frac{\rho}{D}},$$

and λ^2 is the eigenvalue.

The corresponding non-dimensional shear forces, bending and twisting moments become

$$\begin{aligned}
M_\xi &= \frac{\partial \psi_\xi}{\partial \xi} + \frac{\nu}{\phi}\frac{\partial \psi_\eta}{\partial \eta}, \\
M_\eta &= \frac{\partial \psi_\eta}{\partial \eta} + \nu\phi\frac{\partial \psi_\xi}{\partial \xi}, \\
M_{\xi\eta} &= \frac{1}{\phi}\frac{\partial \psi_\xi}{\partial \eta} + \frac{\partial \psi_\eta}{\partial \xi}, \\
Q_\xi &= \psi_\xi + \frac{\partial W}{\partial \xi}, \\
Q_\eta &= \psi_\eta + \frac{1}{\phi}\frac{\partial W}{\partial \eta}.
\end{aligned} \tag{2.17}$$

2.2 Boundary Conditions

Four types of classical boundary conditions and the non-classical elastic one in their dimensionless form, which have been studied thoroughly in the literature, e.g., [5], [12] and [13], are presented here. In all the following expressions of boundary conditions, we take those on the edge y = b or η = 1 as an illustrative example.

2.2.1 Simply Supported Edge

For a simply supported edge at η = 1, we have

$$W = 0,$$

$$\psi_\xi = 0, \tag{2.18}$$

$$M_\eta = 0.$$

Using equations (2.17), the third condition becomes

$$M_\eta = \frac{\partial \psi_\eta}{\partial \eta} = 0. \tag{2.19}$$

Hence, the boundary conditions for a simply supported edge at $\eta = 1$ are

$$W = 0,$$

$$\psi_\xi = 0, \tag{2.20}$$

$$\frac{\partial \psi_\eta}{\partial \eta} = 0.$$

2.2.2 Clamped Edge

The boundary conditions for a clamped edge at $\eta = 1$ are

$$W = 0,$$

$$\psi_\eta = 0, \tag{2.21}$$

$$\psi_\xi = 0.$$

2.2.3 Free Edge

For a free edge at $\eta = 1$, we have

$$M_\eta = 0,$$

$$M_{\xi\eta} = 0, \tag{2.22}$$

$$Q_\eta = 0.$$

Using equations (2.17), these conditions become

$$\frac{\partial \psi_\eta}{\partial \eta} + \nu\phi \frac{\partial \psi_\xi}{\partial \xi} = 0,$$

$$\frac{1}{\phi}\frac{\partial \psi_\xi}{\partial \eta} + \frac{\partial \psi_\eta}{\partial \xi} = 0, \tag{2.23}$$

$$\psi_\eta + \frac{1}{\phi}\frac{\partial W}{\partial \eta} = 0.$$

2.2.4 Slip Shear Edge

The slip shear support requires that the edge is free of transverse shear forces and twisting moments. In addition, the plate cross-section lying along such a boundary, cannot rotate about an axis parallel to the edge. This kind of boundary condition is of a type that would rarely be encountered along the edges of an actual plate. Nonetheless, it will serve as a valuable mathematical device in analyzing plate vibration problems by the superposition method. For a slip shear edge at $\eta = 1$, we have

$$M_{\xi\eta} = 0,$$

$$Q_\eta = 0, \tag{2.24}$$

$$\psi_\eta = 0.$$

Considering equations (2.17), these boundary conditions become

$$\frac{1}{\phi}\frac{\partial \psi_\xi}{\partial \eta} + \frac{\partial \psi_\eta}{\partial \xi} = 0,$$

$$\frac{\partial W}{\partial \eta} = 0, \tag{2.25}$$

$$\psi_\eta = 0.$$

2.2.5 Elastic Edge

Along an elastic edge at $\eta = 1$ with translational and rotational (bending and twisting) restraints, the following three equilibrium conditions must be satisfied

$$M_\eta + K_R \psi_\eta = 0,$$

$$Q_\eta + K_L W = 0, \tag{2.26}$$

$$M_{\xi\eta} + K_T \psi_\xi = 0.$$

where K_R, K_L and K_T are dimensionless bending, translational, and twisting stiffness coefficients, respectively, which are defined in Nomenclature.

Using equations (2.17), those conditions become

$$\frac{\partial \psi_\eta}{\partial \eta} + \nu\phi \frac{\partial \psi_\xi}{\partial \xi} + K_R \psi_\eta = 0,$$

$$\psi_\eta + \frac{1}{\phi} \frac{\partial W}{\partial \eta} + K_L W = 0, \tag{2.27}$$

$$\frac{1}{\phi} \frac{\partial \psi_\xi}{\partial \eta} + \frac{\partial \psi_\eta}{\partial \xi} + K_T \psi_\xi = 0.$$

Chapter 3

The Superposition Method for Analyzing Rectangular Plates Resting on Uniform Elastic Edge Supports

In chapter 2, we developed the governing differential equations for isotropic thick plates. Now, we exploit the superposition method to obtain accurate solutions for the natural frequencies and mode shapes of these plates with elastic supports uniformly distributed along edges.

3.1 Mathematical Procedure

The superposition method described in reference [12] is employed in the present study. Essentially, one obtains exact Levy type solutions for a number of rectangular plate forced vibration problems (building blocks). Each is driven by a harmonic edge rotation or lateral displacement distributed along one edge. After superimposing these solutions, we obtain a system of homogeneous algebraic equations constraining the driving coefficients so that the assembled blocks satisfy the prescribed boundary conditions. The eigenvalues are those values of the dimensionless frequencies which permit a non-trivial solution for the homogeneous equations. In the problem under study here, twelve building blocks are required. They are represented schematically in Figure A.2. Only the first three are described in detail since the steps required to obtain solutions to the other nine will be obvious.

3.1.1 First Building Block

The solution for the first building block is actually obtained in a manner identical to that described in reference [6]. The first building block is driven by a harmonic edge rotation (bending) distributed

along the edge $\eta = 1$. The amplitude of this distributed edge rotation is expressed in series form as

$$\psi_\eta = \sum_{l=0,1}^{\infty} E_l \cos l\pi\xi . \tag{3.1}$$

In addition, this driven edge is free of transverse shear force and twisting moment. The other three non-driven edges are given slip shear supports. This type of supports are indicated in the figure by two small circles adjacent to the edges.

We have the option here of driving the building block instead with a distributed harmonic bending moment. It is found preferable to utilize distributed harmonic edge rotation when analyzing plates with free edges. One thereby avoids the problem of uncovering false eigenvalues (rejection mode eigenvalues) as discussed by Gorman [5].

Levy type solutions are obtained for each of the independent variables, W, ψ_ξ, ψ_η. The trigonometric functions in the following expressions are selected so that the boundary conditions at extremities of their arguments will be satisfied, as required by Levy solution. We therefore write

$$W(\xi,\eta) = \sum_{l=0,1}^{\infty} X_l(\eta)\cos l\pi\xi , \tag{3.2}$$

$$\psi_\xi(\xi,\eta) = \sum_{l=1,2}^{\infty} Y_l(\eta)\sin l\pi\xi , \tag{3.3}$$

$$\psi_\eta(\xi,\eta) = \sum_{l=0,1}^{\infty} Z_l(\eta)\cos l\pi\xi . \tag{3.4}$$

Substituting the above expressions for the plate lateral displacement and rotation functions into the governing differential equations (2.15), we obtain, for $l \geq 1$, the following set of coupled ordinary homogeneous differential equations which are written in matrix form as

$$\begin{Bmatrix} X_l'' \\ Y_l'' \\ Z_l'' \end{Bmatrix} + \begin{bmatrix} 0 & 0 & a_{l1} \\ 0 & 0 & a_{l2} \\ a_{l3} & a_{l4} & 0 \end{bmatrix} \begin{Bmatrix} X_l' \\ Y_l' \\ Z_l' \end{Bmatrix} + \begin{bmatrix} b_{l1} & b_{l2} & 0 \\ b_{l3} & b_{l4} & 0 \\ 0 & 0 & b_{l5} \end{bmatrix} \begin{Bmatrix} X_l \\ Y_l \\ Z_l \end{Bmatrix} = \begin{Bmatrix} 0 \\ 0 \\ 0 \end{Bmatrix}, \tag{3.5}$$

where the primes indicate differentiation with respect to the variable η.

Performing the above substitution, it is found that, for the problem under study, the matrix elements become

$$\begin{aligned} a_{l1} &= \phi, \\ a_{l2} &= -\frac{\phi v_2 (l\pi)}{v_1}, \\ a_{l3} &= -\frac{v_3 \phi}{\phi_h^{\,2}}, \\ a_{l4} &= \phi v_2 (l\pi), \end{aligned} \tag{3.6}$$

and

$$\begin{aligned} b_{l1} &= [\frac{\lambda^4 \phi_h^{\,2}}{v_3} - (l\pi)^2]\phi^2, \\ b_{l2} &= (l\pi)\phi^2, \\ b_{l3} &= \frac{\phi^2 v_3 (l\pi)}{v_1 \phi_h^{\,2}}, \\ b_{l4} &= \frac{\phi^2}{v_1}[\frac{\lambda^4 \phi_h^{\,2}}{12} - (l\pi)^2 - \frac{v_3}{\phi_h^{\,2}}], \\ b_{l5} &= \phi^2[\frac{\lambda^4 \phi_h^{\,2}}{12} - v_1 (l\pi)^2 - \frac{v_3}{\phi_h^{\,2}}]. \end{aligned} \tag{3.7}$$

We now seek solutions for the functions $X_l(\eta)$, $Y_l(\eta)$ and $Z_l(\eta)$, for $l \geq 1$. Introducing the symbol D to indicate differentiation with respect to η, we find that the three equations of matrix equations (3.5) can be written as

$$(D^2 + b_{l1})X_l(\eta) + b_{l2}Y_l(\eta) + a_{l1}DZ_l(\eta) = 0, \tag{3.8}$$

$$b_{l3}X_l(\eta) + (D^2 + b_{l4})Y_l(\eta) + a_{l2}DZ_l(\eta) = 0, \tag{3.9}$$

$$b_{l3}DX_l(\eta) + a_{l4}DY_l(\eta) + (D^2 + b_{l5})Z_l(\eta) = 0. \tag{3.10}$$

Operating on these equations with judiciously selected operations, and combining equations (3.8) and (3.9), and then (3.8) and (3.10), we can easily arrive at a pair of equations from which the quantity $Z_l(\eta)$ is eliminated. These two equations are

$$[a_{l2}(D^2 + b_{l1}) - a_{l1}b_{l3}]X_l(\eta) + [a_{l2}b_{l1} - a_{l1}(D^2 + b_{l4})]Y_l(\eta) = 0 \tag{3.11}$$

and

$$[(D^2 + b_{l5})(D^2 + b_{l1}) - a_{l1}a_{l3}D^2]X_l(\eta) + [b_{l2}(D^2 + b_{l5}) - a_{l1}a_{l4}D^2]Y_l(\eta) = 0. \tag{3.12}$$

We are now in a position to combine equations (3.11) and (3.12) in order to obtain an ordinary differential equation involving one of the independent variables, only. It has been found to be highly desirable by Gorman and Ding [6], from a computational point of view, to eliminate the variable $X_l(\eta)$.

After eliminating the variable $X_l(\eta)$ the ordinary differential equation governing the variable $Y_l(\eta)$ may be written as

$$(D^6 + \alpha_{11}D^4 + \alpha_{22}D^2 + \alpha_{33})Y_l(\eta) = 0, \tag{3.13}$$

where

$$\alpha_{11} = -\frac{\alpha_3 - \alpha_1\alpha_4 - \alpha_6\alpha_7}{\alpha_4},$$

$$\alpha_{22} = -\frac{\alpha_3\alpha_1 - \alpha_2\alpha_4 - \alpha_9}{\alpha_4}, \tag{3.14}$$

$$\alpha_{33} = -\frac{\alpha_3\alpha 2 - \alpha_5\alpha_8}{\alpha_4},$$

and

$$\alpha_1 = b_{11} + b_{15} - a_{11}a_{13},$$

$$\alpha_2 = b_{11}b_{15},$$

$$\alpha_3 = a_{12}b_{12} - a_{11}b_{14},$$

$$\alpha_4 = a_{11},$$

$$\alpha_5 = a_{12}b_{11} - a_{11}a_{13}, \tag{3.15}$$

$$\alpha_6 = a_{12},$$

$$\alpha_7 = b_{12} - a_{11}a_{14},$$

$$\alpha_8 = b_{12}b_{15},$$

$$\alpha_9 = \alpha_6\alpha_8 + \alpha_5\alpha_7.$$

We look on the characteristic equation related to equation (3.13) as a cubic equation with associated roots R_1, R_2 and R_3. For isotropic materials, theoretical discussions put forth by Cleghorn and Yu [4], indicate these roots will always be real although they may be positive or negative. One of these roots is obtained through a numerical search. Denoting the first root as R_1, the other roots become

$$R_2 = -\frac{\alpha_{11} + R_1 - XX}{2}, \tag{3.16}$$

$$R_3 = -\frac{\alpha_{11} + R_1 + XX}{2}, \tag{3.17}$$

where

$$XX = (\alpha_{11} + R_1)^2 + \frac{4\alpha_{33}}{R_1}. \tag{3.18}$$

Now, redesignating the roots R_1, R_2 and R_3 if necessary, so that $R_1 > R_2 > R_3$, we introduce α, β and γ associated with each value of I where

$$\alpha = \sqrt{|R_1|},$$

$$\beta = \sqrt{|R_2|}, \tag{3.19}$$

$$\gamma = \sqrt{|R_3|}.$$

It will be appreciated that associated with negative values of R_1, R_2 and R_3, there will be a pair of solutions involving trigonometric functions. Conversely, associated with positive values, there will be a pair of hyperbolic functions. It is found expedient at this time to introduce a case number which decides which path the computations are to follow. The parameter "case" is assigned values as follows

$$\begin{aligned}
&\text{case} = 1: \qquad R_1,\ R_2 \text{ and } R_3 < 0, \\
&\text{case} = 2: \qquad R_1,\ R_2 < 0,\ R_3 > 0, \\
&\text{case} = 3: \qquad R_1 < 0,\ R_2 \text{ and } R_3 > 0, \\
&\text{case} = 4: \qquad R_1,\ R_2 \text{ and } R_3 > 0.
\end{aligned} \tag{3.20}$$

It will be apparent from the prescribed boundary conditions, at the edge $\eta = 0$, that the functions $X_l(\eta)$ and $Y_l(\eta)$ must be symmetric with respect to the ξ-axis. Similar reasoning allows us to conclude that the functions $Z_l(\eta)$ must be antisymmetric with respect to the same axis. This means that $X_l(\eta)$ and $Y_l(\eta)$ are even functions of η, and $Z_l(\eta)$ is an odd function of η. We are thus able to eliminate three of the six constants associated with each function. For illustrative purposes, we consider the solution when case = 1. We then have

$$Y_l(\eta) = A_l \cos \alpha\eta + B_l \cos \beta\eta + C_l \cos \gamma\eta . \tag{3.21}$$

Of course, had the case been equal to two, the last term of equation (3.21) would have involved cosh $\gamma\eta$. It is not difficult to write solutions associated with other case numbers.

Because of the coupling of the three differential equations, solutions similar in form to equation (3.21) can be written for functions $X_l(\eta)$ and $Z_l(\eta)$. For the situation, case = 1, they take the form

$$X_l(\eta) = A_l R_{l1} \cos \alpha\eta + B_l R_{l2} \cos \beta\eta + C_l R_{l3} \cos \gamma\eta , \tag{3.22}$$

$$Z_l(\eta) = A_l S_{l1} \sin \alpha\eta + B_l S_{l2} \sin \beta\eta + C_l S_{l3} \sin \gamma\eta . \tag{3.23}$$

Similar forms of these equations exist for the other case numbers. It is now necessary to develop expressions for the quantities R_{l1}, S_{l1}, etc..

Consider the first terms of equations (3.21) and (3.22). Substituting them into equation (3.11) and performing differentiation indicated, it is easily shown that

$$R_{11} = \frac{a_{11}(b_{14} - \alpha^2) - a_{12}B_{12}}{a_{12}(b_{11} - \alpha^2) - a_{11}b_{13}}. \tag{3.24}$$

Identical expressions are obtained for R_{12} and R_{13} of equation (3.22), where α is replaced by β and γ, respectively. Expressions for R_{11}, R_{12} and R_{13} for other case numbers are obtained in an identical fashion.

The functions $Y_l(\eta)$ and $Z_l(\eta)$ may be uniquely related by combining equations (3.8) and (3.10) and eliminating the function $X_l(\eta)$. We then obtain

$$[a_{13}b_{12} - a_{14}(D^2 + b_{11})]DY_l(\eta) - [D^4 - (a_{13}a_{11} - b_{11} - b_{15})D^2 + b_{11}b_{15}]Z_l(\eta) = 0 . \tag{3.25}$$

Focusing now on the first term of equations (3.22) and (3.23), and substituting them into equation (3.25), we obtain

$$S_{11} = -\frac{[a_{14}\alpha^2 - (a_{14}b_{11} - a_{13}b_{12})]\alpha}{\alpha^4 + \alpha^2(a_{13}a_{11} - b_{11} - b_{15}) + b_{11}b_{15}}. \tag{3.26}$$

Expressions for S_{11}, S_{12} and S_{13} for other case numbers are obtained in an identical fashion.

Finally, in order to solve for the response of the building block in terms of the Fourier driving coefficients, with $l \geq 1$, it is necessary to establish values for the coefficients A_l, B_l, etc., of the above equations. Focusing attention on the edge, $\eta = 1$, of the first building block, we require that the twisting moment $M_{\xi\eta}$ and the transverse shear force Q_η should vanish. This is in keeping with Mindlin plate boundary conditions as discussed by Dawe and Raoufaeil [13].

We look on the condition $Q_\eta|_{\eta=1} = 0$ first. Utilizing the expression of Q_η provided in (2.17) and considering the solution (3.2), (3.4), (3.22) and (3.23), we obtain

$$A_l(S_{l1} - \frac{\alpha}{\phi}R_{l1})\sin\alpha + B_l(S_{l2} - \frac{\beta}{\phi}R_{l2})\sin\beta + C_l(S_{l3} - \frac{\gamma}{\phi}R_{l3})\sin\gamma = 0. \tag{3.27}$$

Similarly, from the second condition $M_{\xi\eta}|_{\eta=1} = 0$, we have

$$A_l(\frac{\alpha}{\phi} - l\pi S_{l1})\sin\alpha + B_l(\frac{\beta}{\phi} - l\pi S_{l2})\sin\beta + C_l(\frac{\gamma}{\phi} - l\pi S_{l3})\sin\gamma = 0. \tag{3.28}$$

After solving the above two equations (3.27) and (3.28), we obtain B_l and C_l in terms of A_l as

$$\begin{aligned} B_l &= X_1 A_l, \\ C_l &= X_2 A_l, \end{aligned} \tag{3.29}$$

where

$$\begin{aligned} X_1 &= -\frac{[(\frac{\alpha}{\phi}R_{l1} + l\pi S_{l1})(S_{l3} - \frac{\gamma}{\phi}) - (\frac{\gamma}{\phi}R_{l3} + l\pi S_{l3})(S_{l1} - \frac{\alpha}{\phi})]\sin\alpha}{[(\frac{\beta}{\phi}R_{l2} + l\pi S_{l2})(S_{l3} - \frac{\gamma}{\phi}) - (\frac{\gamma}{\phi}R_{l3} + l\pi S_{l3})(S_{l2} - \frac{\beta}{\phi})]\sin\beta}, \\ X_2 &= -\frac{(S_{l1} - \frac{\alpha}{\phi})\sin\alpha + X_1(S_{l2} - \frac{\beta}{\phi})\sin\beta}{(S_{l3} - \frac{\gamma}{\phi})\sin\gamma}. \end{aligned} \tag{3.30}$$

We now may rewrite expression (3.23) as

$$Z_l(\eta) = A_l(S_{l1}\sin\alpha\eta + X_1 S_{l2}\sin\beta\eta + X_2 S_{l3}\sin\gamma\eta). \tag{3.31}$$

Next, enforcing the condition of matching of the imposed edge rotation, equation (3.1), and the parameter ψ_η, equation (3.4), along the driven edge, we obtain

$$E_l = A_l(S_{ll}\sin\alpha + X_1 S_{l2}\sin\beta + X_2 S_{l3}\sin\gamma). \tag{3.32}$$

Denoting the quantity within braces on the right side of equation (3.32) as X_3,

$$X_3 = S_{ll}\sin\alpha + X_1 S_{l2}\sin\beta + X_2 S_{l3}\sin\gamma, \tag{3.33}$$

then we have

$$A_l = \frac{E_l}{X_3}. \tag{3.34}$$

Considering (3.29) and (3.34), the expressions (3.21), (3.22) and (3.23) for $X_l(\eta)$, $Y_l(\eta)$ and $Z_l(\eta)$ become

$$\begin{aligned} X_l(\eta) &= \frac{E_l}{X_3}(R_{ll}\cos\alpha\eta + X_1 R_{l2}\cos\beta\eta + X_2 R_{l3}\cos\gamma\eta), \\ Y_l(\eta) &= \frac{E_l}{X_3}(\cos\alpha\eta + X_1\cos\beta\eta + X_2\cos\gamma\eta), \\ Z_l(\eta) &= \frac{E_l}{X_3}(S_{ll}\sin\alpha\eta + X_1 S_{l2}\sin\beta\eta + X_2 S_{l3}\sin\gamma\eta). \end{aligned} \tag{3.35}$$

There is no difficulty in developing similar expressions for solutions with case = 2, 3 and 4.

We thus have available an analytical solution for the first building block driven by a harmonic distributed edge rotation where the Fourier subscript $l \geq 1$. Before going further, we must examine the case when $l = 0$, which is a simpler problem where the first building block is driven by a single uniformly distributed harmonic edge rotation.

This is essentially a strip problem. The response of the first building block to this uniform harmonic edge rotation will be a function of the dimensionless space variable η. Only two equilibrium differential equations are applicable,

$$\frac{\partial^2 W}{\partial \eta^2} + \phi \frac{\partial^2 \psi_\eta}{\partial \eta^2} + \frac{\lambda^4 \phi^2 \phi_h^{\,2} W}{\nu_3} = 0,$$
$$\frac{\partial^2 \psi_\eta}{\partial \eta^2} - \frac{\nu_3 \phi^2}{\phi_h^{\,2}}\left(\psi_\eta + \frac{1}{\phi}\frac{\partial W}{\partial \eta}\right) + \frac{\lambda^4 \phi^2 \phi_h^{\,2} \psi_\eta}{12} = 0. \tag{3.36}$$

The independent variables W and ψ_η, both functions of η, are written as

$$W(\eta) = X(\eta),$$
$$\psi_\eta(\eta) = Z(\eta). \tag{3.37}$$

We therefore have, following the earlier nomenclature and substituting (3.37) into (3.36),

$$X''(\eta) + a_{01} Z'(\eta) + b_{01} X(\eta) = 0,$$
$$Z''(\eta) + a_{03} X'(\eta) + b_{05} Z(\eta) = 0, \tag{3.38}$$

which are the one-dimensional counterpart of equations (3.5) and

$$a_{01} = \phi,$$
$$a_{02} = -\frac{\nu_3 \phi}{\phi_h^{\,2}},$$
$$b_{01} = \frac{\lambda^4 \phi^2 \phi_h^{\,2}}{\nu_3}, \tag{3.39}$$

$$b_{05} = \frac{\lambda^4 \phi^2 \phi_h^2}{12} - \frac{v_3 \phi^2}{\phi_h^2}.$$

Again, introducing the differential operator D, we have

$$\begin{aligned} (D^2 + b_{01})X(\eta) + a_{01}DZ(\eta) &= 0, \\ a_{03}DX(\eta) + (D^2 + b_{05})Z(\eta) &= 0. \end{aligned} \tag{3.40}$$

Here, we choose to eliminate the quantity $Z(\eta)$ from equations (3.40) and obtain

$$(D^4 + \alpha_{11}D^2 + \alpha_{22})X(\eta) = 0, \tag{3.41}$$

where

$$\begin{aligned} \alpha_{11} &= b_{05} + b_{01} - a_{01}a_{03}, \\ \alpha_{22} &= b_{05}b_{01}. \end{aligned} \tag{3.42}$$

The characteristic equation associated with equation (3.41) may be considered as a quadratic equation with roots R_1 and R_2.

We now have three possible cases as follows

$$\begin{aligned} &\text{case} = 1: && R_1 \text{ and } R_2 < 0, \\ &\text{case} = 2: && R_1 < 0,\ R_2 > 0, \\ &\text{case} = 3: && R_1 \text{ and } R_2 > 0. \end{aligned} \tag{3.43}$$

Designating the roots in such a way that $R_1 < R_2$, and introducing

$$\alpha = \sqrt{|R_1|},$$
$$\beta = \sqrt{|R_2|}, \tag{3.44}$$

we write for case = 1

$$X(\eta) = A_0 \cos \alpha\eta + B_0 \cos \beta\eta,$$
$$Z(\eta) = A_0 S_{01} \sin \alpha\eta + B_0 S_{02} \sin \beta\eta, \tag{3.45}$$

with similar expressions involving hyperbolic and trigonometric functions or hyperbolic functions only for case = 2 and case = 3, respectively. Again, two of the constants have been eliminated because of the boundary conditions along the edge $\eta = 0$.

Following the same steps as described earlier, we are able to develop expressions for the quantities S_{01} and S_{02},

$$S_{01} = -\frac{b_{01} - \alpha^2}{a_{01}\alpha},$$
$$S_{02} = -\frac{b_{01} - \beta^2}{a_{01}\beta}. \tag{3.46}$$

Enforcing the boundary conditions along the edge $\eta = 1$, we obtain

$$B_0 = X_1 A_0, \tag{3.47}$$

where

$$X_1 = -\frac{(\frac{\alpha}{\phi} - S_{01})\sin\alpha}{(\frac{\beta}{\phi} - S_{02})\sin\beta}. \tag{3.48}$$

Matching the imposed edge rotation with the variable ψ_η along the driven edge, we obtain

$$A_0 = \frac{E_0}{X_3}, \tag{3.49}$$

where

$$X_3 = S_{01}\alpha\cos\alpha + X_1 S_{02}\beta\cos\beta. \tag{3.50}$$

Finally, we can express $X(\eta)$ and $Z(\eta)$ as

$$\begin{aligned} X(\eta) &= \frac{E_0}{X_3}(\cos\alpha\eta + X_1\cos\beta\eta), \\ Z(\eta) &= \frac{E_0}{X_3}(S_{01}\sin\alpha\eta + X_1 S_{02}\sin\beta\eta). \end{aligned} \tag{3.51}$$

Similar expressions can be obtained for the other two cases.

3.1.2 Second and Third Building Blocks

The second building block differs from the first one in that it is driven by a harmonic edge twisting rotation and has zero bending moment and shear force along the edge $\eta = 1$. The amplitude of this distributed edge rotation is expressed in series form as

$$\psi_\xi = \sum_{m=1,2}^{\infty} E_m \sin m\pi\xi. \tag{3.52}$$

We also have the option here of driving the building block instead with a distributed harmonic twisting moment. But it is preferable to utilize distributed harmonic edge rotation for the same reason as indicated for the first building block.

The Levy type solutions are written as

$$W(\xi,\eta) = \sum_{m=0,1}^{\infty} X_m(\eta)\cos m\pi\xi, \tag{3.53}$$

$$\psi_\xi(\xi,\eta) = \sum_{m=1,2}^{\infty} Y_m(\eta)\sin m\pi\xi, \tag{3.54}$$

$$\psi_\eta(\xi,\eta) = \sum_{m=0,1}^{\infty} Z_m(\eta)\cos m\pi\xi. \tag{3.55}$$

Following the same steps as those for the first building block, we obtain

$$X_m(\eta) = A_m R_{m1}\cos\alpha\eta + B_m R_{m2}\cos\beta\eta + C_m R_{m3}\cos\gamma\eta, \tag{3.56}$$

$$Y_m(\eta) = A_m\cos\alpha\eta + B_m\cos\beta\eta + C_m\cos\gamma\eta, \tag{3.57}$$

$$Z_m(\eta) = A_m S_{m1}\sin\alpha\eta + B_m S_{m2}\sin\beta\eta + C_m S_{m3}\sin\gamma\eta, \tag{3.58}$$

where R_{m1}, S_{m1}, etc. have the same expressions as R_{11}, S_{11}, etc.. and α, β, γ have the same definitions as given before.

Along the driven edge, $\eta = 1$, we require that the shear force Q_η and the bending moment M_η should vanish.

We look on the condition $M_\eta|_{\eta=1} = 0$ first. Utilizing the expression of M_η provided in (2.17) and considering the equations (3.54), (3.55), (3.57) and (3.58), we obtain

$$A_m(\alpha S_{m1} + m\pi\nu\phi)\cos\alpha + B_m(\beta S_{m2} + m\pi\nu\phi)\cos\beta + C_m(\gamma S_{m3} + m\pi\nu\phi)\cos\gamma = 0. \tag{3.59}$$

Similarly, from the second condition $Q_\eta|_{\eta=1} = 0$ we can obtain

$$A_m(S_{m1} - \frac{\alpha}{\phi}R_{m1})\sin\alpha + B_m(S_{m2} - \frac{\beta}{\phi}R_{m2})\sin\beta + C_m(S_{m3} - \frac{\gamma}{\phi}R_{m3})\sin\gamma = 0. \quad (3.60)$$

After solving the above two equations (3.59) and (3.60), we obtain B_m and C_m in terms of A_m as

$$\begin{aligned} B_m &= X_1 A_m, \\ C_m &= X_2 A_m, \end{aligned} \quad (3.61)$$

where

$$X_1 = -\frac{(S_{m1} - \frac{\alpha}{\phi}R_{m1})(\gamma S_{m3} + m\pi\nu\phi)\sin\alpha - (S_{m3} - \frac{\gamma}{\phi}R_{m3})(\alpha S_{m1} + m\pi\nu\phi)\cos\alpha\tan\gamma}{(S_{m2} - \frac{\beta}{\phi}R_{m2})(\gamma S_{m3} + m\pi\nu\phi)\sin\beta - (S_{m3} - \frac{\gamma}{\phi}R_{m3})(\beta S_{m2} + m\pi\nu\phi)\cos\beta\tan\gamma},$$

$$X_2 = -\frac{(\alpha S_{m1} + m\pi\nu\phi)\cos\alpha + X_1(\beta S_{m2} + m\pi\nu\phi)\cos\beta}{(\gamma S_{m3} + m\pi\nu\phi)\cos\gamma}. \quad (3.62)$$

We now may rewrite expression (3.56) as

$$X_m(\eta) = A_m(R_{m1}\cos\alpha\eta + X_1R_{m2}\cos\beta\eta + X_2R_{m3}\cos\gamma\eta). \quad (3.63)$$

Next, enforcing the condition of matching of the imposed edge rotation, equation (3.52), and the parameter ψ_ξ, equation (3.54), along the driven edge, we obtain

$$E_m = A_m(\cos\alpha + X_1\cos\beta + X_2\cos\gamma). \quad (3.64)$$

Denoting the quantity within braces on the right side of equation (3.64) as X_3,

$$X_3 = \cos\alpha + X_1\cos\beta + X_2\cos\gamma, \quad (3.65)$$

then we have

$$A_m = \frac{E_m}{X_3}. \tag{3.66}$$

Considering (3.61) and (3.66), the expressions (3.56), (3.57) and (3.58) for $X_m(\eta)$, $Y_m(\eta)$, and $Z_m(\eta)$ become

$$\begin{aligned} X_m(\eta) &= \frac{E_m}{X_3}(R_{m1}\cos\alpha\eta + X_1R_{m2}\cos\beta\eta + X_2R_{m3}\cos\gamma\eta), \\ Y_m(\eta) &= \frac{E_m}{X_3}(\cos\alpha\eta + X_1\cos\beta\eta + X_2\cos\gamma\eta), \\ Z_m(\eta) &= \frac{E_m}{X_3}(S_{m1}\sin\alpha\eta + X_1S_{m2}\sin\beta\eta + X_2S_{m3}\sin\gamma\eta). \end{aligned} \tag{3.67}$$

There is no difficulty in developing similar expressions for solutions with case = 2, 3 and 4.

We thus have obtained an analytical solution for the second building block driven by a harmonic distributed edge twisting where the Fourier subscript m ≥ 1. When m = 0, the second building block actually is not driven.

The third building block differs from the first one only in that it is driven by a harmonic edge displacement and has zero bending and twisting moments along the edge $\eta = 1$. The amplitude of this distributed edge displacement is expressed in series form as

$$W = \sum_{n=0,1}^{\infty} E_n \cos n\pi\xi. \tag{3.68}$$

We also have the option here of driving the building block instead with a distributed harmonic shear force. But it is preferable to utilize distributed harmonic edge displacement for the same reason as indicated for the first building block.

The Levy type solutions are written as

$$W(\xi,\eta) = \sum_{n=0,1}^{\infty} X_n(\eta)\cos n\pi\xi, \tag{3.69}$$

$$\psi_\xi(\xi,\eta) = \sum_{n=1,2}^{\infty} Y_n(\eta)\sin n\pi\xi, \tag{3.70}$$

$$\psi_\eta(\xi,\eta) = \sum_{n=0,1}^{\infty} Z_n(\eta)\cos n\pi\xi. \tag{3.71}$$

Following the same steps as those for the first building block, we obtain

$$X_n(\eta) = A_n R_{n1}\cos\alpha\eta + B_n R_{n2}\cos\beta\eta + C_n R_{n3}\cos\gamma\eta, \tag{3.72}$$

$$Y_n(\eta) = A_n\cos\alpha\eta + B_n\cos\beta\eta + C_n\cos\gamma\eta, \tag{3.73}$$

$$Z_n(\eta) = A_n S_{n1}\sin\alpha\eta + B_n S_{n2}\sin\beta\eta + C_n S_{n3}\sin\gamma\eta, \tag{3.74}$$

where R_{n1}, S_{n1}, etc. have the same expressions as R_{11}, S_{11}, etc.. and α, β, γ have the same definitions as given before.

Along the driven edge, $\eta = 1$, we require that the twisting moment $M_{\xi\eta}$ and the bending moment M_η should vanish.

We look on the condition $M_\eta|_{\eta=1} = 0$ first. Utilizing the expression of M_η provided in (2.17) and considering the solution (3.70), (3.71), (3.73) and (3.74), we obtain

$$A_n(\alpha S_{n1} + n\pi\nu\phi)\cos\alpha + B_n(\beta S_{n2} + n\pi\nu\phi)\cos\beta + C_n(\gamma S_{n3} + n\pi\nu\phi)\cos\gamma = 0. \tag{3.75}$$

Similarly, from the second condition $M_{\xi\eta}|_{\eta=1} = 0$ we can obtain

$$A_n(\frac{\alpha}{\phi} + n\pi S_{n1})\sin\alpha + B_n(\frac{\beta}{\phi} + n\pi S_{n2})\sin\beta + C_n(\frac{\gamma}{\phi} + n\pi S_{n3})\sin\gamma = 0. \tag{3.76}$$

After solving the above two equations (3.75) and (3.76), we obtain B_n and C_n in terms of A_n as

$$B_n = X_1 A_n,$$
$$C_n = X_2 A_n, \tag{3.77}$$

where

$$X_1 = -\frac{(\frac{\alpha}{\phi} + n\pi S_{n1})(\gamma S_{n3} + n\pi\nu\phi)\sin\alpha - (\frac{\gamma}{\phi} + n\pi S_{n3})(\alpha S_{n1} + n\pi\nu\phi)\cos\alpha\tan\gamma}{(\frac{\beta}{\phi} + n\pi S_{n2})(\gamma S_{n3} + n\pi\nu\phi)\sin\beta - (\frac{\gamma}{\phi} + n\pi S_{n3})(\beta S_{n2} + n\pi\nu\phi)\cos\beta\tan\gamma},$$
$$X_2 = -\frac{(\alpha S_{n1} + n\pi\nu\phi)\cos\alpha + X_1(\beta S_{n2} + n\pi\nu\phi)\cos\beta}{(\gamma S_{n3} + n\pi\nu\phi)\cos\gamma}. \tag{3.78}$$

We now may rewrite expression (3.72) as

$$X_n(\eta) = A_n(R_{n1}\cos\alpha\eta + X_1 R_{n2}\cos\beta\eta + X_2 R_{n3}\cos\gamma\eta). \tag{3.79}$$

Next, enforcing the condition of matching of the imposed edge displacement, equation (3.68), and the parameter W, equation (3.69), along the driven edge, we obtain

$$E_n = A_n(R_{n1}\cos\alpha + X_1 R_{n2}\cos\beta + X_2 R_{n3}\cos\gamma). \tag{3.80}$$

Denoting the quantity within braces on the right side of equation (3.80) as X_3,

$$X_3 = R_{n1}\cos\alpha + X_1 R_{n2}\cos\beta + X_2 R_{n3}\cos\gamma, \tag{3.81}$$

then we have

$$A_n = \frac{E_n}{X_3}. \tag{3.82}$$

Considering (3.77) and (3.82), the expressions (3.72), (3.73) and (3.74) for $X_n(\eta)$, $Y_n(\eta)$ and $Z_n(\eta)$ become

$$\begin{aligned} X_n(\eta) &= \frac{E_n}{X_3}(R_{n1}\cos\alpha\eta + X_1R_{n2}\cos\beta\eta + X_2R_{n3}\cos\gamma\eta), \\ Y_n(\eta) &= \frac{E_n}{X_3}(\cos\alpha\eta + X_1\cos\beta\eta + X_2\cos\gamma\eta), \\ Z_n(\eta) &= \frac{E_n}{X_3}(S_{n1}\sin\alpha\eta + X_1S_{n2}\sin\beta\eta + X_2S_{n3}\sin\gamma\eta). \end{aligned} \tag{3.83}$$

There is no difficulty in developing similar expressions for solutions with case = 2, 3 and 4.

We thus have obtained an analytical solution for the third building block driven by a harmonic distributed edge displacement where the Fourier subscript n ≥ 1. When n = 0, the third building block is actually driven by a uniformly distributed harmonic edge displacement. Following the same steps as presented for the first building block, the solution for this case can be obtained easily. It is found almost the same as the one of the first building block except that we have here

$$X_1 = -\frac{\alpha S_{01}\cos\alpha}{\beta S_{02}\cos\beta}, \tag{3.84}$$

$$X_3 = R_{01}\cos\alpha + X_1R_{02}\cos\beta, \tag{3.85}$$

because of the different boundary conditions along the driven edge $\eta = 1$.

3.1.3 Other Building Blocks

The fourth, fifth and sixth building blocks differ from the first three only in that they are driven along

the edge $\xi = 1$. For convenience, we will designate the Fourier driving coefficients for those three building blocks by the symbols E_o, E_p and E_q, respectively. The solutions for the responses of those three building blocks are available from those of the first three provided that we take the following steps [6]

a) replace λ^2 with $\lambda^2\phi^2$,

b) replace ϕ_h with ϕ_h/ϕ,

c) replace ϕ with $1/\phi$,

d) interchange η and ξ.

The solutions of the seventh, eighth and ninth building blocks differ from those of the first three only in that η should be replaced by $1-\eta$. We use r, s and t, respectively, for the Fourier driving coefficient subscripts here.

Similarly, the last three building block solutions are extracted from those of the second three by replacing ξ with $1-\xi$. The Fourier driving coefficients for those three building blocks are designated by E_u, E_v and E_w, respectively.

3.1.4 Eigenvalue Matrix

With the building block solutions available, we are now ready to construct the eigenvalue matrix. The matrix is developed in a manner similar to that described in [12] for thin plates. Such a matrix, based on a three term expansion for each building block, is shown schematically in Figure A.3. The actual number of terms employed can be arbitrarily increased in order to achieve any degree of desired convergence.

Rectangular figures along the right edge of the schematic matrix of Figure A.3 indicate whether the associated group of equations are related to moments or edge force equilibrium and to which edge they pertain. The first group arises because of the requirement to satisfy the bending moment equilibrium condition in (2.27) along the edge $\eta = 1$. Toward this end, all moment and rotation distributions along the edge which are not available in a cosine series are expanded in such a series. Note that we must employ the same number of terms in such a series as in the building block solutions to obtain a square eigenvalue matrix. The first, second and third equations, etc., in the group are then obtained by requiring that the sum of the contributions to the left side of the first equation in (2.27) of each building block must equal zero, for the first, second, third terms, etc., of the series. This gives rise to a set of K+1 homogeneous algebraic equations relating the Fourier driving coefficients E_l, E_m, etc. K equals the upper limit of subscripts in the Fourier expressions.

The second group of equations is due to the requirement to satisfy the twisting moment equilibrium condition along the edge $\eta = 1$. All twisting moment and rotation distributions along the edge which are not available in a sine series are expanded in such a series. Another set of K+1 equations are then obtained by requiring that the sum of the contributions to the left side of the third equation in (2.27) of each building block must equal zero for each term of the sine series.

The third group of equations is due to the requirement to satisfy the vertical edge force equilibrium condition along the edge $\eta = 1$. All shear force and displacement distributions along the edge which are not available in a cosine series are expanded in such a series. The third set of K+1 equations are then obtained by requiring that the sum of the contributions to the left side of the second equation in (2.27) of each building block must equal zero for each term of the cosine series.

It will now be appreciated that, as we continue around the plate in counterclockwise fashion, all of the twelve groups of equations can be written. We thus arrive at a set of 12K+12 equations relating the 12K+12 unknown Fourier driving coefficients. The coefficient matrix of the set of equations forms our eigenvalue matrix. The procedure for computing eigenvalues is well established. First we choose a trial value of λ^2 and compute the determinant of the associated matrix. The trial value is

increased in increments until a value is obtained which causes the matrix determinant to vanish. Higher eigenvalues may then be computed. With an eigenvalue obtained and one of the driving coefficients set equal to unity, a solution for the remaining driving coefficients can be obtained and the associated mode shape plotted.

It is worth noting that with the aid of physical reasoning, much of the work normally required in generating the eigenvalue matrix can be avoided. It will be observed that there is a 4 by 4 array of segments in the matrix of Figure A.3. Let us suppose that the elastic supports are distributed uniformly along all the edges and we have computed the four segments immediately underneath the first three building blocks. An identical computer algorithm can be used to generate the four segments immediately beneath the second three building blocks provided that we make the changes as indicated earlier for generation of the second three building blocks.

There is no need to generate the matrix segments below the other six building blocks. They can be transferred from the segments underneath the first six building blocks, with sign modifications as required. Let us denote the segments by subscripts (i, j). It will be found that the following pairs of matrix segments are identical [6]

segment (1, 1) = segment (3, 3),

segment (3, 1) = segment (1, 3),

segment (4, 4) = segment (2, 2),

segment (2, 4) = segment (4, 2).

Other segments below the last six building blocks may be obtained from the corresponding segments of the first six building blocks by changing signs in the second, fourth rows, etc.,

segment (2, 3) = ±segment (2, 1),

segment (4, 3) = ±segment (4, 1),

segment (1, 4) = ±segment (1, 2),

segment (3, 4) = ±segment (3, 2).

Taking advantage of these observations reduces computer running time and also reduces the possibility of error. It is noted that we need to change the above procedure slightly when the four edges have different stiffness values.

3.2 Computed Results

The eigenvalues and mode shapes of square plates with uniformly distributed elastic supports along all four edges are obtained for illustrative purpose. It should be emphasized that the four edges are allowed to take on different stiffness coefficients in the superposition method.

A value of the parameter κ^2 equal to 0.8601 and Poisson ratio $\nu = 0.3$ used by many researchers are employed in all computations. There are two other very close commonly used values of κ^2, 5/6 and $\pi^2/12$, which were first introduced by Reissner [2] and Mindlin [3], respectively. However in the tests conducted during the present research, it was found that changing the value of κ^2 from 0.8601 to 5/6 or $\pi^2/12$ had no significant effect on the computed eigenvalues.

In running the Fortran codes for the entitled vibration analysis, it is found that the rate of convergence for the first six eigenvalues is excellent. Figure B.1 shows the convergence trend for the fifth vibration modes of square plates. It can be seen that the eigenvalues converge monotonically to the exact values from the low side, while convergence is a little slower for the simply supported plates with $K_R = 0$. However we found that four digits of accuracy for all computed data may be obtained when

ten terms in Levy type solutions are used in the test. Ten term expansions for the plate displacement and rotation functions are therefore utilized in computation.

In order to study the effect of twisting restraint, eigenvalues of the first vibration modes are computed and then plotted in Figure B.2 for simply supported square plates resting on rotational supports with or without twisting restraint. It can be seen that the twisting restraint has more significant effect on thicker plate vibration, particularly when not acting with bending restraint simultaneously. However, its effect is trivial when compared with those of translational and bending restraints.

It is obvious, in view of the numerous parameters involved, that only a very limited amount of data can be presented. The main body of computed results appears in Table B.1 ~ B.3 and Table B.4 ~ B.6 for thin and thicker square plates, respectively. Eigenvalues of first six mode vibration modes are recorded for various rotational and translational stiffnesses. Mode shapes associated with some eigenvalues are plotted In Figure B.3 ~ B.7.

In Table B.7 ~ B.9, first mode eigenvalues computed by the superposition method described here are compared with those reported in reference [14] for thin square plates with various elastic stiffnesses. Comparison is also made between data generated by the present method and corresponding data extracted from the publication of Chung [10] in Table B.10 for simply supported thicker square plates with rotational restraint. It is seen that there is good agreement between those sets of results. Where there are slight differences the results of the present study are seen to be slightly lower. This is to be expected since the Rayleigh-Ritz energy method is used in their analysis.

Finally, tests are conducted to approach the known eigenvalues for plates with classical boundary conditions. The results are presented in Table B.12 and B.13. FFFF, SSSS, and CCCC represent completely free, simply supported, and fully clamped boundary conditions, respectively. In each case the appropriate stiffness coefficients are given values of zero or 100000 to simulate zero or infinite stiffnesses as indicated in Table B.10. It will be noted that all of the limiting cases are approached with no deviations.

Chapter 4

Summary

4.1 Conclusions

In the present study, the superposition method has been used successfully to obtain the accurate analytical solutions for the natural frequencies and mode shapes of shear deformable plates resting on uniformly distributed translational and rotational elastic edge supports. The solutions obtained satisfy the governing differential equations exactly throughout the domain of the plate, and the boundary conditions can be satisfied to any desired degree of accuracy by taking more terms in the slope and displacement solutions. The effects of transverse shear deformation and rotary inertia have been taken into account by means of the first order shear deformation relationship as developed by Mindlin.

The convergence was found excellent and four digits of accuracy was obtained by utilizing ten terms in Levy type solutions. All the three classical boundary conditions, namely, free, simply supported, and clamped, were approached when the stiffness coefficients were allowed to take on appropriate limits. It is well known that the results for Mindlin plate theory must approach those of thin plate theory as plate thickness approaches zero. We therefore compared our results with corresponding thin plate ones and obtained good agreement.

In our study, the effects of twisting edge restraint were investigated for the first time. It was found that the twisting restraint has more significant effect on thicker plate vibration, particularly when not acting with bending restraint simultaneously. However, its effect is trivial when compared with those of translational and bending restraints.

Eigenvalues were tabulated for the first six vibration modes of square plates with various stiffness coefficients and some mode shapes were also plotted. To the author's knowledge, these solutions constitute the first analytical approach to resolve those important plate vibration problem by the superposition method. It is expected that the tabulated eigenvalues may prove useful to designers as well as providing reference values against which future researchers may compare their results.

4.2 Further Research Possibilities

The present research involves rectangular plates with uniformly distributed elastic edge supports. Further research can be extended to the following areas,

(1) Free vibration analysis of rectangular plates with varying elastic edge supports,

(2) Free vibration analysis of composite plates with elastic edge supports,

(3) Applications of higher order shear deformation plate theories for free vibration analysis of thicker plates using superposition method.

Reference

[1] Liew, K. M., Xiang, Y. and Kitipornchai, S., "Research on Thick Plate Vibration: a Literature Survey", Journal of Sound and Vibration, 1995, Vol. 180, pp 163-176.

[2] Reissner, E., "The Effect of Transverse Shear Deformation on the Bending of Elastic Plates", Journal of Applied Mechanics, 1945, Vol. 67, pp A69-77.

[3] Mindlin, R. D., "Influence of Rotary Inertia and Shear on Flexural Motions of Isotropic Elastic Plates", Journal of Applied Mechanics, 1951, Vol. 18, pp 31-38.

[4] Yu, S. D. and Cleghorn, W. L., "Accurate Free Vibration Analysis of Clamped Mindlin Plates Using the Method of Superposition", Proceedings of 11th Symposium on Engineering Applications of Mechanics, University of Regina, Saskatchewan, 1992, pp 226-230.

[5] Gorman, D. J., "Free Vibration Analysis of Rectangular Plates", Elsevier North Holland Inc., New York, 1982.

[6] Gorman, D. J. and Ding, Wei, "Accurate Free Vibration Analysis of the Completely Free Rectangular Mindlin Plate", Journal of Sound and Vibration, 1996, Vol. 189, pp 341-353.

[7] Ding, Wei, "Free Vibration Studies of Shear Deformable Plates by the Traditional Superposition and Superposition-Galerkin Method", Master's Thesis, Department of Mechanical Engineering, University of Ottawa, Ottawa, Ontario, Canada, 1995.

[8] Cleghorn, W. L. and Yu, S. D., "Effect of Shear Deformation on Free Flexural Vibration of Clamped Rectangular Plates", Machinery Dynamics and Element Vibration, 1991, DE-36, pp 185-191.

[9] Yu, S. D. and Cleghorn, W. L., "Accurate Free Vibration Analysis of Clamped Mindlin Plates Using the Method of Superposition", Canadian Society for Mechanical Engineering Journal, 1993, Vol. 17, pp 243-255.

[10] Chung, J. H., Chung, T. Y. And Kim, K. C., "Vibration Analysis of Orthotropic Mindlin Plates with Edges Elastically Restrained against Rotation", Journal of Sound and Vibration, 1993, Vol. 163, pp 151-163.

[11] Saha, K. N., Kar, R. C. and Datta, P. K., "Free Vibration Analysis of Rectangular Mindlin Plates with Elastic Restraints Uniformly Distributed Along the Edges", Journal of Sound and Vibration, 1996, Vol. 192, pp 885-904.

[12] Gorman, D. J., "A General Solution for the Free Vibration of Rectangular Plates Resting on Uniform Elastic Edge Supports", Journal of Sound and Vibration, 1990, Vol. 139, pp 325-335.

[13] Dawe, D. J. and Raoufaeil, O. L., "Rayleigh-Ritz Vibration Analysis of Mindlin Plates", Journal of Sound and Vibration, 1980, Vol. 69, pp 345-359.

[14] Kim, C. S., Young, P. G. And Dickinson, S. M., "On the Flexural Vibration of Rectangular Plates Approached by Using Single Polynomials in the Rayleigh-Ritz Method", Journal of Sound and Vibration, 1990, Vol. 143, pp 379-394.

[15] Mindlin, R. D., Schacknow, A. and Deresiewicz, H., "Flexural Vibrations of Rectangular Plates", Journal of Applied Mechanics, 1956, Vol. 23, pp 430-436.

Appendix A

Illustrative Figures

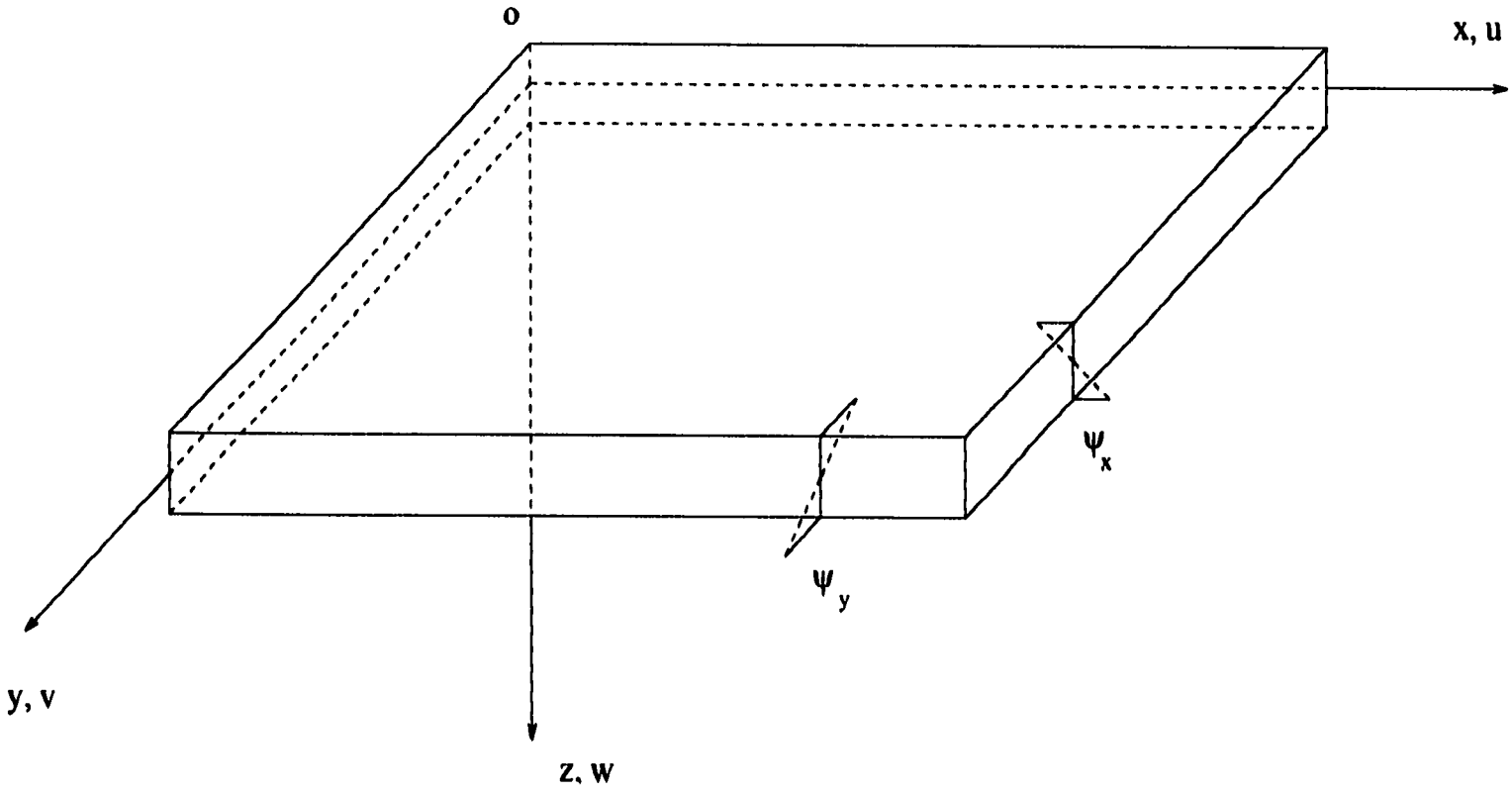

Figure A.1. Plate coordinate system.

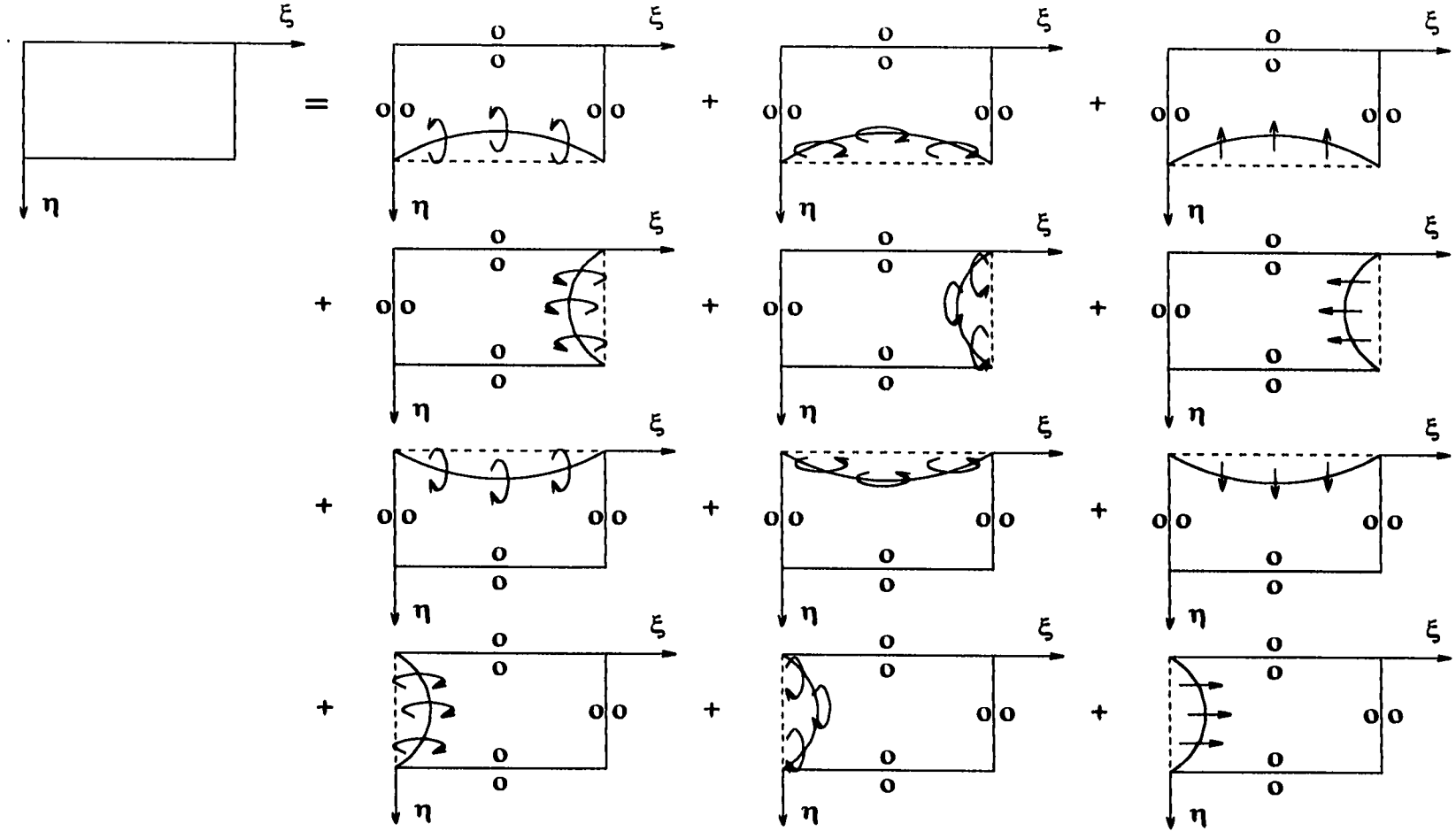

Figure A.2. Schematic representation of forced vibration solutions (building blocks) utilized in free vibration analysis of rectangular Mindlin plates resting on uniformly distributed elastic edge supports.

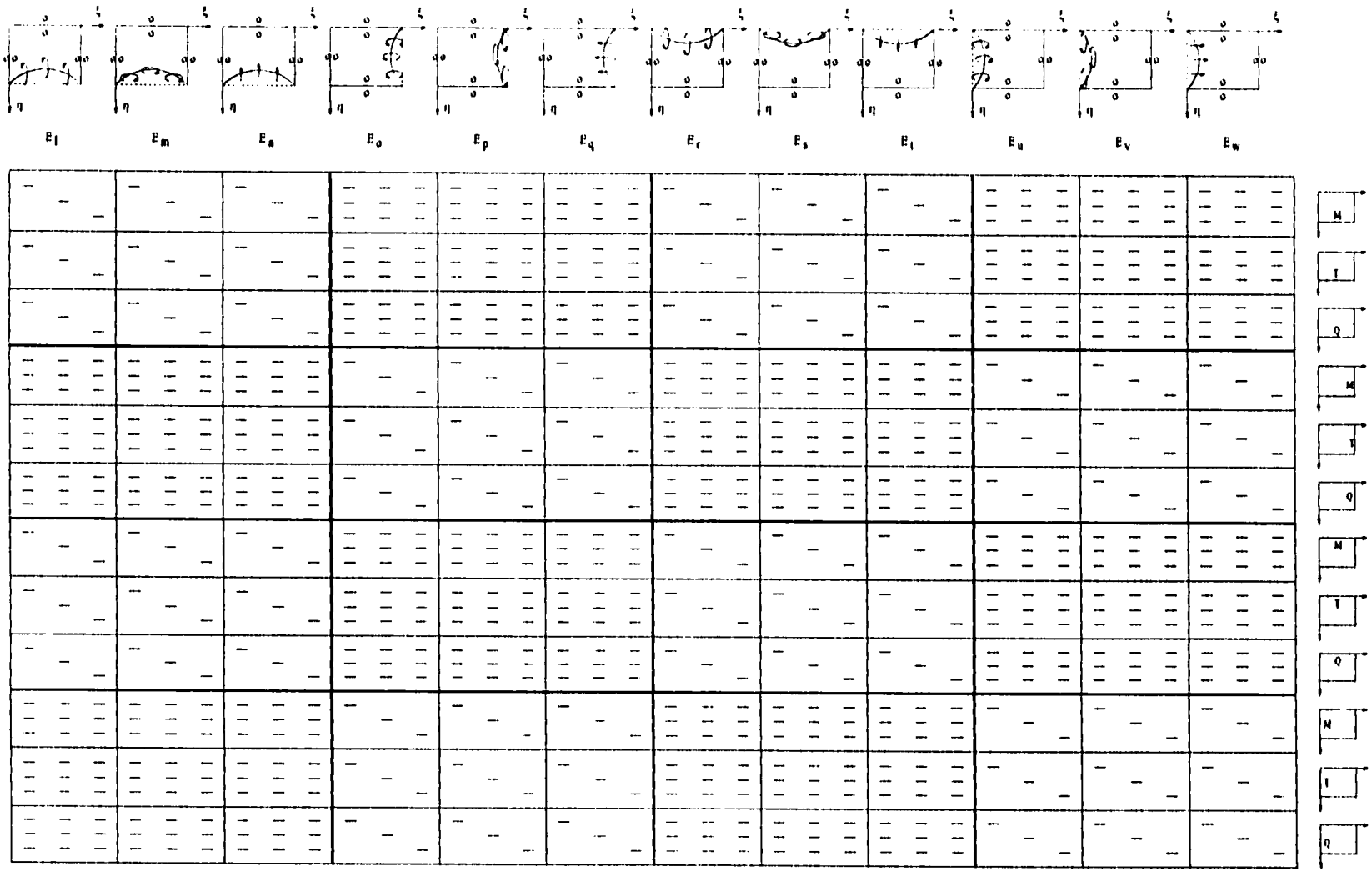

Figure A.3. Schematic representation of eigenvalue matrix generated in free vibration analysis of rectangular Mindlin plates resting on uniformly distributed elastic edge supports.

Appendix B

Computed Eigenvalues and Associated Mode Shapes

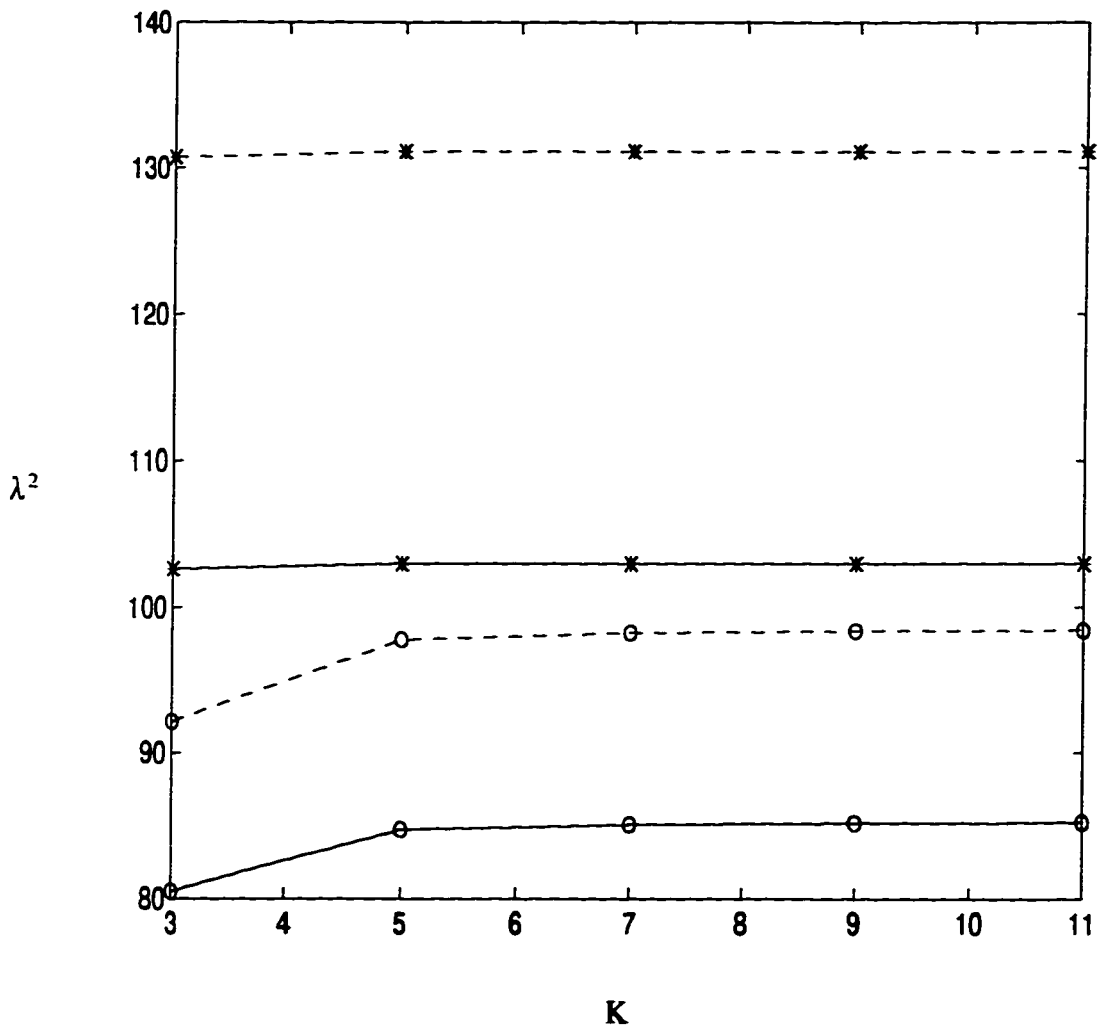

Figure B.1. Convergence trend of the fifth vibration modes of square plates (--: $\phi_h = 0.01$, -: $\phi_h = 0.1$, o: $K_L = K_T = 100000$, $K_R = 0$, *: $K_L = K_T = K_R = 100000$).

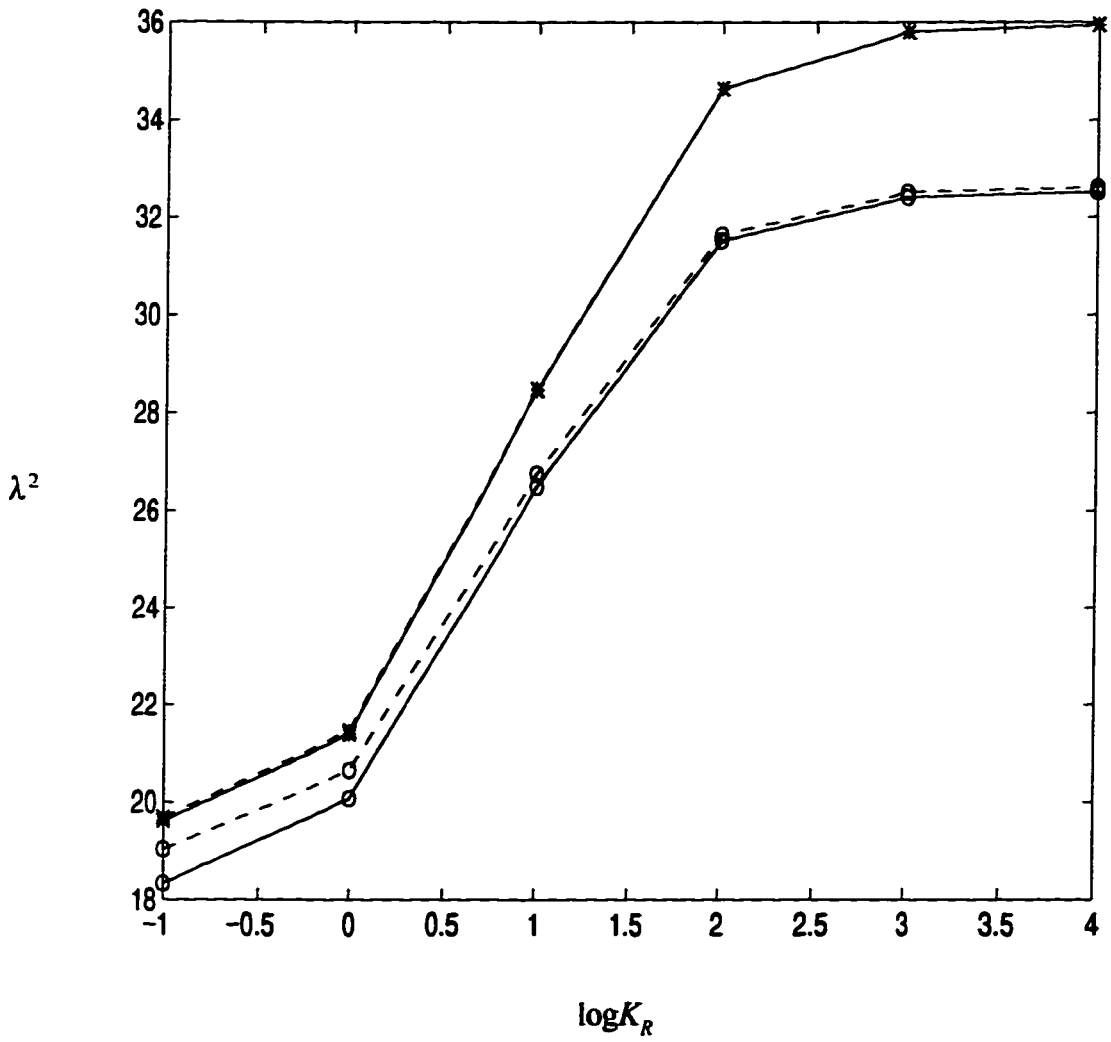

Figure B.2. Effects of twisting rotation restraints on square plate free vibrations (K_L = 100000, *: ϕ_h = 0.01, o: ϕ_h = 0.1, -: K_T = 0, --: K_T = 100000).

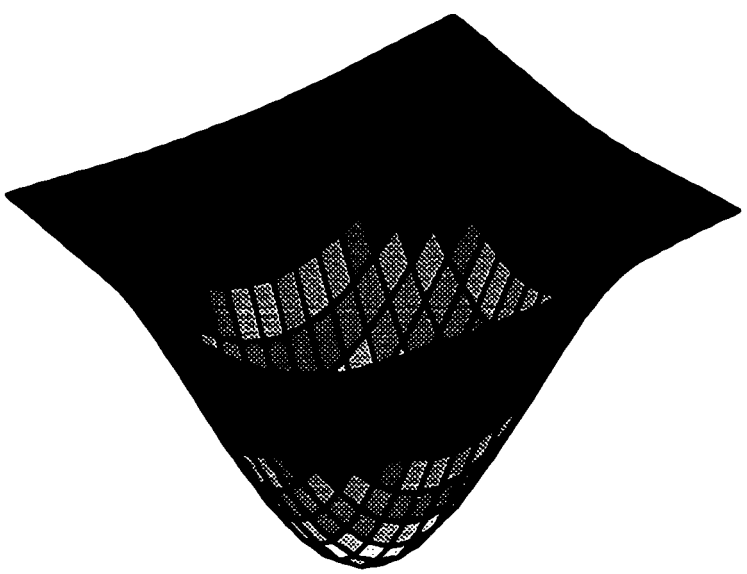

Figure B.3. First vibration mode shape of a thicker square plate ($\phi_h = 0.1$, $K_T = 0$, $K_R = K_L = 10$, $\lambda^2 = 25.78$).

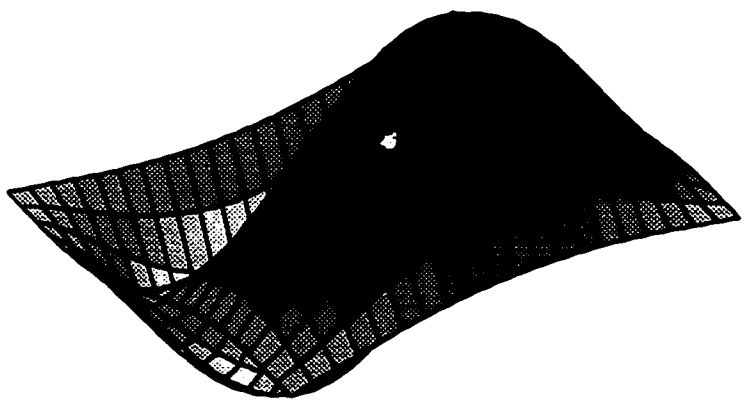

Figure B.4. Second vibration mode shape of a thicker square plate ($\phi_h = 0.1$, $K_T = 0$, $K_R = K_L = 10$, $\lambda^2 = 50.83$).

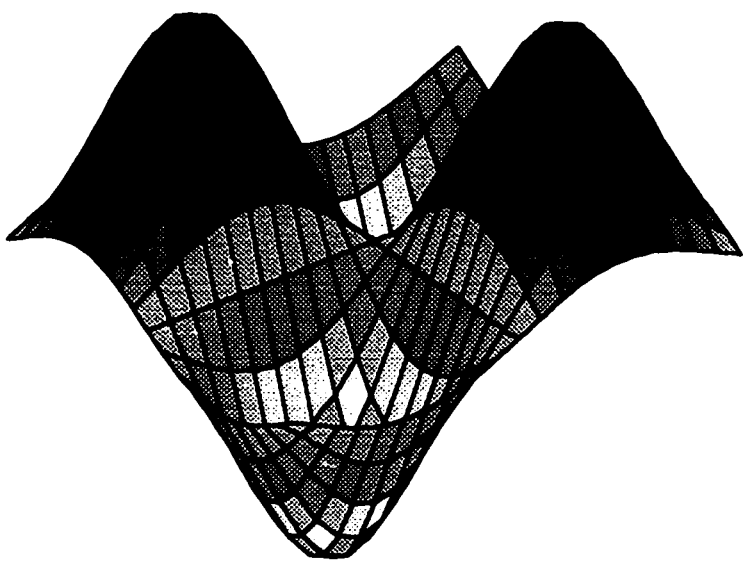

Figure B.5. Fourth vibration mode shape of a thicker square plate ($\phi_h = 0.1$, $K_T = 0$, $K_R = K_L = 10$, $\lambda^2 = 71.67$).

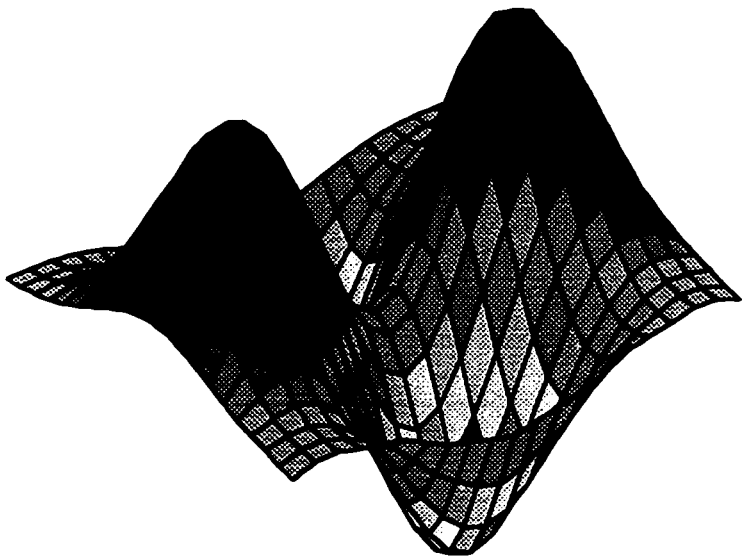

Figure B.6. Fifth vibration mode shape of a thicker square plate ($\phi_h = 0.1$, $K_T = 0$, $K_R = K_L = 10$, $\lambda^2 = 85.83$).

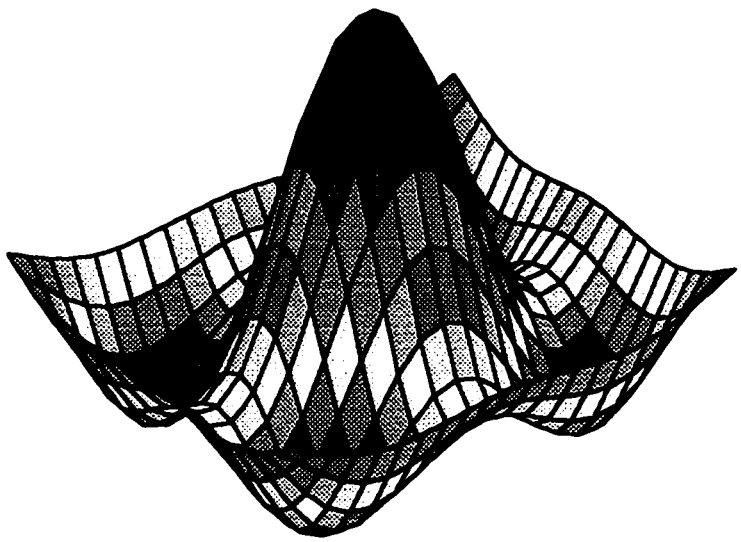

Figure B.7. Sixth vibration mode shape of a thicker square plate ($\phi_h = 0.1$, $K_T = 0$, $K_R = K_L = 10$, $\lambda^2 = 86.82$).

K_L	Mode				
	1	2, 3	4	5	6
0	0	0	13.42	19.59	24.26
0.000001	0.3801	0.5375	13.43	19.60	24.27
0.00001	1.199	1.699	13.57	19.69	24.34
0.0001	3.718	5.350	14.82	20.54	25.00
0.001	9.787	16.13	23.58	27.47	31.25
0.01	16.36	36.31	50.76	58.11	61.58
0.1	19.10	47.89	72.59	91.62	91.75
1	19.57	48.89	77.71	97.54	97.69
100000	19.64	49.14	78.41	98.31	98.37

Table B.1. Eigenvalues for a thin square plate with all four edges resting on equal translational elastic supports with no bending and twisting restraints ($\phi_h = 0.01$, $K_R = K_T = 0$, $\nu = 0.3$, $\kappa^2 = 0.8601$).

K_L, K_R	Mode				
	1	2, 3	4	5	6
0	0	0	13.42	19.59	24.26
0.001	9.787	16.13	23.58	27.47	31.25
0.01	16.38	36.32	50.76	58.11	61.58
0.1	19.30	47.21	72.75	91.77	91.88
1	21.35	50.74	79.60	99.39	99.51
10	28.46	60.05	90.40	110.8	111.0
100	34.64	70.64	104.2	126.6	127.2
1000	35.81	72.96	107.5	130.6	131.2
100000	35.95	73.24	107.9	131.1	131.8

Table B.2. Eigenvalues for a thin square plate with all four edges resting on equal translational and bending supports with no twisting restraints ($\phi_h = 0.01$, $K_T = 0$, $\nu = 0.3$, $\kappa^2 = 0.8601$).

K_R	Mode				
	1	2, 3	4	5	6
0	19.64	49.14	78.41	98.31	98.37
0.01	19.66	49.16	78.44	98.33	98.39
0.1	19.84	49.34	78.62	98.51	98.57
1	21.42	51.00	80.34	100.2	100.3
10	28.47	60.09	90.50	110.9	111.1
100	34.64	70.64	104.2	126.6	127.2
1000	35.81	72.95	107.5	130.6	131.3
10000	35.93	73.21	107.9	131.1	131.7
100000	35.95	73.24	107.9	131.1	131.8

Table B.3. Eigenvalues for a simply supported thin square plate with all four edges subject to equal bending restraints and with no twisting restraints ($\phi_h = 0.01$, $K_L = 100000$, $K_T = 0$, $\nu = 0.3$, $\kappa^2 = 0.8601$).

K_L	Mode				
	1	2, 3	4	5	6
0	0	0	12.73	18.96	23.34
0.0001	0.3801	0.5349	12.75	18.97	23.35
0.001	1.200	1.690	12.89	19.05	23.42
0.01	3.708	5.317	14.19	19.88	24.08
0.1	9.717	15.95	23.05	26.67	30.26
1	15.84	34.79	48.37	55.29	58.32
10	17.99	43.16	64.40	80.37	80.62
100	18.31	44.36	67.24	83.85	83.98
100000	18.34	44.51	67.59	84.24	84.37

Table B.4. Eigenvalues for a thicker square plate with all four edges resting on equal translational elastic supports with no bending and twisting restraints ($\phi_h = 0.1$, $K_R = K_T = 0$, $\nu = 0.3$, $\kappa^2 = 0.8601$).

K_L, K_R	Mode				
	1	2, 3	4	5	6
0	0	0	2.73	18.96	23.34
0.001	1.200	1.690	12.89	19.06	23.42
0.01	3.718	5.338	14.20	19.93	24.11
0.1	9.766	15.99	23.09	26.97	30.43
1	17.15	35.30	48.58	55.50	58.40
10	25.78	50.83	71.67	85.83	86.82
100	31.41	60.10	84.11	99.58	100.7
1000	32.40	61.86	86.50	102.3	103.4
100000	32.52	62.07	86.79	102.6	103.8

Table B.5. Eigenvalues for a thicker square plate with all four edges resting on equal translational and bending supports with no twisting restraints (ϕ_h = 0.1, K_T = 0, ν = 0.3, κ^2 = 0.8601).

K_R	Mode				
	1	2, 3	4	5	6
0	18.34	44.51	67.59	84.24	84.37
0.01	18.36	44.53	67.61	84.25	84.38
0.1	18.54	44.68	67.76	84.38	84.51
1	20.08	46.12	69.16	85.59	85.75
10	26.49	53.31	76.65	92.40	92.90
100	31.52	60.49	84.87	100.6	101.6
1000	32.41	61.90	86.58	102.4	103.5
10000	32.51	62.06	86.77	102.6	103.8
100000	32.52	62.07	86.79	102.6	103.8

Table B.6. Eigenvalues for a simply supported thicker square plate with all four edges subject to equal bending restraints and with no twisting restraints ($\phi_h = 0.1$, $K_L = 100000$, $K_T = 0$, $\nu = 0.3$, $\kappa^2 = 0.8601$).

K_L	2.77E-6	4.43E-5	2.21E-4	2.21E-3	2.21E-2	2.21E-1	2.77E+0	2.77E+5
Kim[14]	0.632	2.503	5.369	12.326	17.819	19.452	19.736	19.739
Present	0.6322	2.503	5.369	12.33	17.77	19.36	19.60	19.64

Table B.7. Comparison of first mode free vibration eigenvalues for thin square plates with all four edges resting on equal translational elastic support with no bending and twisting restraints ($\phi_h = 0.01$, $K_R = K_T = 0$, $\nu = 0.3$, $\kappa^2 = 0.8601$).

K_R	0.1	1	10	20	100	1000	10000	100000
Kim[14]	19.937	21.502	28.502	31.081	34.671	35.843	35.971	35.985
Present	19.84	21.42	28.47	31.05	34.64	35.81	35.93	35.95

Table B.8. Comparison of first mode free vibration eigenvalues for simply supported thin square plates with all four edges subject to equal bending elastic restraint ($\phi_h = 0.01$, $K_L = 100000$, $K_T = 0$, $\nu = 0.3$, $\kappa^2 = 0.8601$).

K_R	0.1	1	5	10	50	100	500	1000	10000	1E+10
K_L	2.77E-6	2.77E-5	1.38E-4	2.77E-4	1.38E-3	2.77E-3	1.38E-2	2.77E-2	2.77E-1	2.77E5
Kim[14]	0.632	1.990	4.401	6.170	13.052	17.337	27.606	30.853	35.336	35.989
Present	0.6322	1.990	4.401	6.170	13.06	17.34	27.59	30.83	35.30	35.95

Table B.9. Comparison of first mode free vibration eigenvalues for thin square plates with all four edges resting on equal bending and translational elastic supports with no twisting restraint ($\phi_h = 0.01$, $K_T = 0$, $\nu = 0.3$, $\kappa^2 = 0.8601$).

K_R	10	50	100	1000
Chung[10] beam functions	26.68	30.70	31.52	32.38
Chung[10] polynomials	26.70	30.72	31.56	32.42
Present	26.49	30.67	31.52	32.41

Table B.10. Comparison of first mode free vibration eigenvalues for simply supported thicker square plates with all four edges subject to equal bending elastic restraint ($\phi_h = 0.1$, $K_L = 100000$, $K_T = 100000$, $\nu = 0.3$, $\kappa^2 = 0.8601$).

Boundary condition	K_L	K_R	K_T
Free	0	0	0
Simply supported	100000	0	100000
Clamped	100000	100000	100000

Table B.11. K_L, K_R, and K_T values for free, simply supported, and clamped boundary conditions.

Case designation	FFFF	SSSS	CCCC
Actual eigenvalue	24.41 Gorman[6]	98.52 Mindlin[15]	131.8 Yu[4]
Approached value	24.26 (24.41, v = 0.333)	98.52	131.8
Deviation (%)	0.00	0.00	0.00

Table B.12. Comparison between sixth mode free vibration eigenvalues for thin square plates with classical boundary conditions and those approached as limiting cases with the present analysis (ϕ_h = 0.01, ν = 0.3, κ^2 = 0.8601).

Case designation	FFFF	SSSS	CCCC
Actual eigenvalue	23.45 Gorman[6]	85.30 Mindlin[15]	103.9 Yu[4]
Approached value	23.34 (23.45, v = 0.333)	85.30	103.9
Deviation (%)	0.00	0.00	0.00

Table B.13. Comparison between sixth mode free vibration eigenvalues for thicker square plates with classical boundary conditions and those approached as limiting cases with the present analysis ($\phi_h = 0.1$, $\nu = 0.3$, $\kappa^2 = 0.8601$).